Title

Endocannabinoids produced in photoreceptor cells in response to light activate Drosophila TRP channels

Journal

Science Signaling, 15(755)

ISSN

1945-0877

Authors

Sokabe, Takaaki
Bradshaw, Heather B
Tominaga, Makoto
et al.

Publication Date

2022-10-11

DOI

10.1126/scisignal.abl6179

Peer reviewed

Endocannabinoids produced in photoreceptor cells in response to light activate *Drosophila* TRP channels

Authors: Takaaki Sokabe[1,2,3*†], Heather B. Bradshaw[4], Makoto Tominaga[2,3], Emma Leishman[4], Avinash Chandel[1], and Craig Montell[1,*]

Affiliations: [1]Department of Molecular, Cellular, and Developmental Biology and the Neuroscience Research Institute, University of California, Santa Barbara; California 93106, USA.

[2†]Division of Cell Signaling, National Institute for Physiological Sciences, and Thermal Biology Group, Exploratory Research Center on Life and Living Systems (ExCELLS), National Institutes of Natural Sciences; Okazaki, Aichi, 444-8787, Japan.

[3†]Department of Physiological Sciences, SOKENDAI; Okazaki, Aichi, 444-8787, Japan.

[4]Department of Psychological and Brain Sciences, Indiana University; Bloomington, Indiana, 47405, USA.

[*]Corresponding authors.

Email addresses: sokabe@nips.ac.jp (TS); cmontell@ucsb.edu (CM)

Abstract:

Drosophila phototransduction is a model for signaling cascades that culminate with the activation of Transient Receptor Potential (TRP) cation channels. TRP and TRPL are the canonical TRP (TRPC) channels that are regulated by light stimulation of rhodopsin and engagement of $G\alpha_q$ and phospholipase $C\beta$ (PLC). Lipid metabolite(s) generated downstream of PLC are essential for the activation of the TRPC channels in photoreceptor cells, and various mechanisms have been proposed. We sought to identify the key lipids produced subsequent to PLC stimulation that contribute to channel activation. Here, using genetics, lipid analysis and Ca^{2+} imaging, we found that light increased the amount of an abundant endocannabinoid, 2-linoleoyl glycerol (2-LG), in vivo. The increase in 2-LG amounts depended on the PLC and diacylglycerol lipase (DAGL) encoded by *norpA* and *inaE*, respectively. This endocannabinoid facilitated TRPC-dependent Ca^{2+} influx in a heterologous expression system and in dissociated ommatidia from compound eyes. Moreover, 2-LG and mechanical stimulation cooperatively activated TRPC channels in ommatidia. We propose that 2-LG is a physiologically relevant endocannabinoid that activates TRPC channels in photoreceptor cells.

One Sentence Summary: An endocannabinoid, 2-linoleoylglycerol, increased upon light stimulation in a phospholipase C- and diacylglycerol lipase-dependent manner, and stimulated the TRP and TRPL channels in in *Drosophila* photoreceptor cells.

INTRODUCTION

Phototransduction is crucial in animals ranging from worms to humans because it enables reception of visual information from the surrounding environment, positive or negative phototaxis, and entrainment of circadian rhythms. In some photoreceptor cells, such as mammalian rods and cones, the phototransduction cascade culminates with closing of cyclic nucleotide gated cation channels (*1*). In contrast, the cascades in *Drosophila* photoreceptor cells and in mammalian intrinsically photosensitive retinal ganglion cells lead to opening of transient receptor potential (TRP) cation channels (*1-3*).

In *Drosophila*, the main site for light reception and transduction is the compound eye, which is comprised of ~800 repeat units called ommatidia. A single ommatidium harbors eight photoreceptor cells, each of which includes a rhabdomere. This specialized portion of the photoreceptor cells consists of thousands of microvilli, thereby enabling rhodopsin to be expressed at very high levels for efficient photon capture (*1-3*). The *Drosophila* phototransduction cascade has been studied for over 50 years beginning with the seminal work by Pak and colleagues (*4*). This has led to elucidation of the critical signaling proteins that transduce light into an electrical signal (*3, 5*). Light-activation of rhodopsin engages a heteromeric $G\alpha_q$ protein and stimulation of the phospholipase C (PLC) encoded by *norpA* (*6*), which in turn induces opening of Ca^{2+} permeable cation channels. These include the TRP channel, which is the classical member of the TRP family (*7, 8*), and a second canonical TRP channel (TRPC), TRPL (*9-11*). Related TRP channels are conserved from flies to humans (*12, 13*). In addition,

Drosophila phototransduction involves mechanisms underlying the dynamic movements of signaling proteins, as well as proteins that function in the visual cycle, post-translational modification of signaling proteins, and the composition of the signalplex, which is a large macromolecular assembly that clusters together many of the key proteins that function in phototransduction through interactions with the PDZ-containing protein, INAD (*2, 3, 5*). The fly eye is also an outstanding tissue to model human diseases (*14-19*).

Stimulation of PLC is essential for activation of the TRP and TRPL channels. However, the mechanism linking activity of PLC to opening of TRP and TRPL is still unresolved. PLC hydrolyzes phosphatidylinositol 4,5-bisphosphate (PIP_2) to release inositol phosphate 1,4,5 trisphosphate (IP_3), a H^+ and diacylglycerol (DAG) (*1-3*). Consistent with this conclusion, light exposure causes a decrease in PIP_2 levels and an increase in DAG in fly heads (*20*). IP_3 and the release of Ca^{2+} from the endoplasmic reticulum does not seem to play a role in *Drosophila* phototransduction (*21, 22*) and multiple other models have been proposed. According to one study, PIP_2 depletion accompanied by local intracellular acidification by H^+ promotes channel activation (*23*). DAG has also been reported to activate TRP and TRPL in excised rhabdomeric membranes (*24-26*). Mechanical contraction of the rhabdomeral membrane has been proposed to contribute to channel activation (*27*), which may occur due to cleavage of the head group of PIP_2, leaving the smaller lipid, DAG, in the membrane (*27*). Polyunsaturated fatty acids (PUFAs) have been reported to activate TRP and TRPL (*26,*

28, 29), although another study showed that PUFAs do not increase with illumination (*25*).

To identify physiologically relevant lipids that could activate TRP and TRPL, we performed a lipid analysis using fly heads exposed to light or that were maintained in the dark. We found that several lipids increased in concentration upon light stimulation in control flies but not in the *norpA* mutant that lack the PLC required for phototransduction. The lipids that were increased by light included two endocannabinoid species. Endocannabinoids are related to plant-derived cannabinoids, which in mammals can activate the same receptors as cannabinoids, such as the G-protein coupled receptors (GPCRs) CB1 and CB2 (*30*). However, *Drosophila* has no CB1 and CB2 homologs (*31*), and no cannabinoid receptor has been identified in flies. We found that one endocannabinoid, 2-linoleoyl glycerol (2-LG), which was ~60—100 times more abundant than the other lipids, increased upon light stimulation, and was nearly absent in either the light or dark in a mutant, *inaE*, that disrupts a DAG lipase. 2-LG activated TRPL channels in vitro in a dose-dependent manner and induced Ca^{2+} influx in dissociated ommatidia through TRP and TRPL channels. We propose that 2-LG is a key lipid that contributes to activation of the TRPC channels in photoreceptor cells. Moreover, activation of the TRPC channels by 2-LG is enhanced by mechanical stimulation, which is one of the proposed mechanisms for activating these channels (*27*).

RESULTS

Endocannabinoid levels are increased by light

To evaluate lipids that are increased by light stimulation of *Drosophila* photoreceptor cells, we performed lipid analyses (Fig. 1A). In addition to using control flies (w^{1118}) maintained in the dark or stimulated with light, we also analyzed $norpA^{P24}$ mutant flies (in a w^{1118} background) to identity light-induced changes in lipid levels that were PLC-dependent. Half the control and $norpA^{P24}$ flies were then exposed to blue light for 5 minutes because the major rhodopsin in the compound eyes (rhodopsin 1) is maximally activated by 480 nm light (*32*). We used whole heads mechanically separated from the bodies for the following lipid analyses because the retina represents a substantial proportion (~20%) of the mass of the heads.

To quantify the amounts of lipid metabolites in each sample, we used liquid chromatography-tandem mass spectrometry (LC/MS/MS). We analyzed 14 lipids that are produced in *Drosophila* larvae (*33*), and which we could reliably identify in *Drosophila* heads in our preliminary studies. These included lipids that are known or could potentially depend on PLC for their biosynthesis because PLC activity is required for the light response. PLC hydrolyzes PIP_2 to generate IP_3, H^+ and DAG. DAG can be metabolized by DAGL to 2-LG (Fig. 1B and S1A) and other 2-monoacylglycerols (2-MAGs). In mammals, 2-MAGs such as 2-arachidonoyl glycerol (2-AG) function as endocannabinoids (*30*) and 2-LG activates and binds to mammalian CB1 when it is ectopically expressed in *Drosophila* (*34*). We did not include long PUFAs (C20 and C22) such as arachidonic acid (C20:4) because they do not appear to be synthesized in *Drosophila* (*33, 35, 36*).

Three of the lipids that we characterized displayed significant changes in control fly heads. Most prominent among these three was the endocannabinoid 2-LG (Fig. 1C and Data file S1). The 30% light-dependent rise in 2-LG levels in control heads did not occur in *norpA*^{P24} heads (Fig. 1C) demonstrating that the change in 2-LG levels was PLC-dependent. In contrast to 2-LG, we did not detect significant light-dependent changes in two other 2-MAGs analyzed: 2-palmitoyl glycerol (2-PG) and 2-oleoyl glycerol (2-OG; fig. S1, B and C). During a 10 second light exposure, the increase in 2-LG amounts was not quite at the threshold for statistical significance (Fig. 1D). Therefore, we continued lipid analysis after 5-minute exposure to light, which offered greater sensitivity and technical ease. Control flies also exhibited a light-dependent increase in the anandamide-related lipid linoleoyl ethanolamide (LEA; Fig. 1E). However, the absolute levels of LEA were ~100 fold lower than 2-LG (Fig. 1, C and E). Light did not impact the concentration of LEA in *norpA*^{P24} flies (Fig. 1E). We also quantified a possible precursor of LEA, phospho-LEA (*37*), and found a similar light-dependent rise in phospho-LEA (Fig. 1F), which was present at low levels comparable to LEA (Fig. 1E). There was a small, non-significant light-induced increase in phospho-LEA in *norpA*^{P24} flies (Fig. 1F). In contrast to LEA and phospho-LEA, light did not significantly affect the biosynthesis of other types of *N*-acyl ethanolamides, including those that contained a saturated fatty acid, such as stearoyl ethanolamide (S-EA, C18:0) and palmitoyl ethanolamide (P-EA, C16:0; fig. S1, D and E). We also did not detect a significant light-dependent change in the concentrations of oleoyl ethanolamide (O-EA), which is conjugated to the monosaturated fatty acid, oleic acid (OA, C18:1; fig. S1F) or OA itself (fig. S1G).

We observed a light-induced increase of the N-acyl glycine (NAG) linoleoyl glycine that was not quite statistically significant (LinGly; fig. S1H). As with LEA and phospho-LEA, the absolute levels of LinGly were much lower than 2-LG (Fig. 1C and S1H). The concentrations of all three other NAG molecules analyzed were not impacted by light (fig. S1, I to K). Thus, all four lipids that displayed light-dependent increases and a tendency of increase were conjugated to linoleic acid (LA). However, LA showed only a modest, statistically insignificant increase in light-stimulated control flies (fig. S1L). A previous lipid analysis focusing on PUFAs found that none of the PUFAs analyzed, including LA, changed in the presence of light (*25*). Thus, even though several reports implicate PUFAs as activators of TRP and TRPL (*26, 28, 29*), the effects may not be physiologically relevant. Also consistent with previous studies (*35, 36*), we did not detect arachidonic acid in any of our samples. Together, our data indicate that light stimulation promotes biosynthesis of LA-containing endocannabinoids and the precursor in a PLC-dependent manner.

Because 2-LG is the major lipid produced by light, we tested whether the generation of this endocannabinoid depended on *inaE*, which encodes a DAG lipase that functions in phototransduction (*34, 38*). When $inaE^{N125}$ flies were maintained in the dark, the level of 2-LG was low and reduced ~20-fold relative to the control (Fig. 1G and S2A). Moreover, stimulation of the mutant with blue light did not cause an increase in 2-LG (Fig. 1G). Similarly, the amounts of LEA and LinGly in dark-maintained $inaE^{N125}$ flies were not upregulated by light stimulation. However, in contrast to 2-LG, the levels of these lipids and were not significantly different from dark-maintained control flies (fig.

S2, B and C). These results indicate that *inaE* contributes to the production of 2-LG as reported (*34*) and is necessary for the light-dependent increase.

We also evaluated 2-LG levels after exposing flies to a different light paradigm. Blue light (480 nm) converts a large amount of rhodopsin 1 to metarhodopsin 1, which remains active even after cessation of the light stimulus (*39*). However, orange light (580 nm) not only activates rhodopsin 1, but also converts metarhodopsin 1 back to rhodopsin 1, thereby quickly abolishing the photoreceptor response when the light shuts off (*39*). We stimulated w^{1118} control flies with blue light for 6 minutes, which was followed by 30 seconds in the dark. We also exposed the flies to blue light for 5 minutes, which was followed by orange light for 1 minute, and then maintained the flies in the dark for 30 seconds. Upon blue light stimulation following by darkness, the 2-LG level was lower than the dark control, while after blue and orange light stimulation followed by darkness, the 2-LG level was comparable to the dark control. (fig. S2D). Based on these results, we conclude that 2-LG is metabolized following cessation of blue light because phototransduction continues.

Endocannabinoids activate TRPL and mammalian TRPC channels in vitro

To test whether the linoleoyl conjugates that rise in concentration in response to light increase channel activity in vitro, we focused on TRPL because TRP is largely retained in the endoplasmic reticulum in tissue cultures and has been refractory to functional characterization. We used a *Drosophila* cell line (Schneider 2 cells; S2 cells) that contains an integrated *trpl::GFP* gene that can be induced with $CuSO_4$ (*40*). Cells that

are not exposed to $CuSO_4$ do not express *trpl::GFP* and provide a negative control. We used different lipids to stimulate cells loaded with a cell permeant, ratiometric Ca^{2+} indicator (Fura-2 AM) and determined the increase in intracellular Ca^{2+} (Ca^{2+}_i). Finally, we exposed the cells to the ionophore ionomycin to determine the maximum possible increase in Ca^{2+}, which we calculated by normalizing the maximum value with each treatment relative to the ionomycin response.

We performed dose-response analyses for the endocannabinoids (2-LG and LEA) and LinGly over a 1000-fold concentration range (100 nM—100 μM). We did not include phospho-LEA in these experiments because it is amphipathic and will not flip to the inner leaflet of the plasma membrane when added to the bath solution. Cells not exposed to $CuSO_4$ and that did not express TRPL did not respond to 2-LG even at the highest concentration tested (Fig. 2A and S3A). In contrast, 2-LG robustly stimulated an increase in Ca^{2+}_i in cells exposed to $CuSO_4$ and expressing TRPL with an EC_{50}=5.23 μM (Fig. 2, A to D). 100 μM 2-LG induced Ca^{2+}_i that was 51.5 ± 3.3% of the maximum possible value (Fig. 2, A to C). LEA and LinGly also stimulated an increase in Ca^{2+}_i in TRPL-expressing cells (EC_{50} μM: LEA=7.04, LinGly=2.99; Fig. 2, A and D to F), but not in cells not expressing TRPL (Fig. 2A and S3, B and C). In contrast to the efficacy of these linoleoyl conjugates in stimulating a rise in Ca^{2+}_i in TRPL-positive cells, a membrane-permeable analogue of DAG, 1-oleoyl-2-acetyl-*sn*-glycerol (OAG), was not effective at inducing Ca^{2+}_i increase (Fig. 2A and S3D). OA was also ineffective at activating TRPL (Fig. 2A and S3E) consistent with the lack of increase in OA level upon light stimulation (fig. S1G).

Because 2-LG, LEA and LinGly contain LA in their structures, channel activation might result from generation of LA either by hydrolysis or degradation. Indeed, LA activated a TRPL-dependent elevation in Ca^{2+}_i (Fig. 2A and S3, F and G). To assess whether generation of LA from 2-LG, LEA and LinGly activates TRPL, we tested the effects of addition of the MAG lipase inhibitor JZL 184 or the MAG lipase/fatty acid amide hydrolase inhibitor IDFP (*41, 42*). We found that neither inhibitor reduced Ca^{2+}_i (Fig. 3A), supporting the idea that the endocannabinoids (2-LG and LEA) and NAG promote TRPL activation.

LA is generated in *Drosophila*, but arachidonic acid is not detectable in vivo unless it is supplied in the diet. Nevertheless, we examined the effects of 2-arachidonoyl glycerol (2-AG) and found that it evoked Ca^{2+}_i increases in TRPL-expressing cells (fig. S4, A and D). We tested a stable 2-AG analog, 2-AG ether (*43*), which also evoked Ca^{2+}_i increase (fig. S4, B and E). Anandamide (AEA) is similar in structure to LEA. The stable AEA analog methanandamide (*44*) also stimulated a rise in Ca^{2+}_i in TRPL-expressing cells (fig. S4, C and F). Thus, arachidonic acid conjugates stimulate TRPL. Because the stable 2-AG analogs activate TRPL to a comparable extent as 2-AG, this supports the idea that endocannabinoids themselves rather than PUFA metabolites are sufficient to activate TRPL.

2-LG and LEA increase upon light stimulation in vivo. Therefore, we assessed whether there were synergistic or additive effects resulting from applying mixtures of these lipids. We tested all combinations of 2-LG, LEA, LinGly and LA while maintaining the same total concentration (6 μM). We did not observe either synergistic or additive

effects on the increase in Ca^{2+}_i relative to the same concentration of the single lipids (Fig. 3, B to D).

Mammalian homologs of *Drosophila* TRPC channels are regulated by PIP_2 metabolites (*45, 46*). To assess whether 2-LG activates mammalian TRPC channels, we used Fura-2 to evaluate the Ca^{2+} responses of HEK293 cells transiently expressing mouse TRPC5 or TRPC6. We exposed the cells to 2-LG, then to either riluzole or GSK1702934A, which are non-lipid activators of TRPC5 and TRPC6, respectively (*47, 48*), and finally with ionomycin. 2-LG induced significant Ca^{2+} increases in TRPC5- and TRPC6-expressing HEK293 cells compared with the vector-transfected cells, although the responsiveness varied among the cells (Fig. 4, A to F).

Endocannabinoids act on TRP and TRPL channels in ommatidia

To address whether the endocannabinoid 2-LG activates TRP and TRPL in photoreceptor cells, we isolated ommatidia from flies (fig. S5A) that expressed the genetically encoded Ca^{2+} sensor GCaMP6f in six out of the eight photoreceptor cells under control of the *rhodopsin 1* (*ninaE*) promotor (*ninaE>GCaMP6f*) (*49*). We performed all analyses in a $norpA^{P24}$ genetic background to prevent light activation of the TRP and TRPL channels. We stimulated the ommatidia with 2-LG, then with ionomycin to confirm that the ommatidia were viable. We assessed an increase in Ca^{2+} by dividing the change in fluorescence by basal fluorescence ($\Delta F/F_0$).

We focused primarily on 2-LG because it is the most abundant lipid that is induced by light. When we applied 2-LG to the bath solution, we observed an increase in Ca^{2+} in

norpA^{P24} photoreceptor cells (Fig. Fig. 5A and S5B). Because the *norpA*^{P24} mutation removes the PLC required for phototransduction, the change in fluorescence was not due to light stimulation. We introduced the *norpA*^{P24} mutation into a genetic background that removes both TRP and/or TRPL (*norpA*^{P24};*trpl*^{302};*trp*^{343}, *norpA*^{P24};+;*trp*^{343}, or *norpA*^{P24};*trpl*^{302};+) and found that only ommatidia from *norpA*^{P24};*trpl*^{302};trp^{343} showed significantly lower responses to 2-LG, which was significant from *norpA*^{P24};+;+ control (Fig. 5, B to H, and S5C and D). The statistical significance of this reduction did not depend on the two outliers in the *norpA*^{P24};+;+ control (Fig. 5G) because the difference was still statistically significant in the absence of these two values. In further support of the conclusion that the TRPC channels are activated by 2-LG in vivo, the percentage of no or low responding ommatidia (max $\Delta F/F_0 \leq 0.2$) was 3.85 times higher in the mutant lacking TRPL and TRP (*norpA*^{P24};*trpl*^{302};*trp*^{343}) compared with the control (Fig. 5I; *norpA*^{P24};+;+).

The reduction in fluorescence ($\Delta F/F_0$) in *norpA*^{P24};*trpl*^{302};*trp*$^{343.}$ flies suggested that the rise in $\Delta F/F_0$ was due to TRP and TRPL. Elimination of just TRP or TRPL resulted in only small differences from the *norpA*^{P24} control, which were not statistically significant (Fig. 5, E to I). The minimal changes upon elimination of just TRP or TRPL were consistent with electrophysiological analyses showing that the loss of TRPL alone has virtually no effect on the amplitude of the light response (*10*), whereas the removal of TRP has only minimal effects on the response amplitude under dim or moderate light conditions (*50, 51*). The 2-LG induced an increase in $\Delta F/F_0$ only in the presence and not the absence of Ca^{2+} in the bath solution (Fig. 5, J and K), demonstrating that the

increase in GCaMP6f fluorescence was due to Ca^{2+} influx and not to release of Ca^{2+} from internal stores. The $Ca^{2+}{}_I$ increase induced by application of 2-LG to *norpA*^{P24} ommatidia was significantly suppressed in the presence of ruthenium red (RuR), a TRP channel blocker (Fig. 5L). This reduction in $Ca^{2+}{}_i$ was comparable to that induced by eliminating TRPL and TRP in the *norpA*^{P24};*trpl*^{302};*trp*^{343} mutant (Fig. 5G). The $Ca^{2+}{}_i$ was increased to the level comparable to the *norpA*^{P24} control after RuR washout (Fig. 5, G and L). These results support the idea that 2-LG stimulates $Ca^{2+}{}_i$ increase through TRP and TRPL.

We also examined whether LEA and LinGly stimulated a rise in $Ca^{2+}{}_i$. We found that these lipids induced $Ca^{2+}{}_i$ increases in *norpA*^{P24} control flies, which were significantly higher than those in *norpA*^{P24};*trpl*^{302};*trp*^{343} flies (Fig. 5, M and N). In the absence of the one outlier for LinGly, the statistical significance was essentially unchanged. Consistent with previous data indicating that LA but not OA is effective in activating the TRPC channels (*26, 28*), we found that LA activated ommatidia at a level similar to that of 2-LG, whereas OA evoked only a minimal Ca^{2+} increase similar to that observed in ommatidia lacking TRPL and TRP (Fig. S5E).

2-LG and mechanical stimulation cooperatively activate TRP and TRPL in vivo

TRP and TRPL channels are proposed to be mechanically activated by contraction of photoreceptor cells (*27*). This appears to be caused by PIP_2 hydrolysis, leaving a smaller lipid product (DAG) in the membrane (*27*). Although our data indicated that 2-LG was sufficient to activate TRP and TRPL, they do not exclude the possibility that

mechanical stimulation functions together with 2-LG. Therefore, we evaluated whether or not a combination of 2-LG and mechanical stimulation results in greater activation of TRP and TRPL than each stimulation alone. To mechanically stimulate the ommatidia, we switched the bath from an isotonic solution (~316 mOsm) to a hypotonic solution (~216 mOsm). This manipulation induced a transient increase in $Ca^{2+}{}_i$ in *norpA*^{P24} control ommatidia, which was significantly reduced in *norpA*^{P24};*trpl*^{302};*trp*^{343} mutant ommatidia lacking TRPL and TRP (Fig. 6, A to C). The Ca^{2+} responses to hypotonic stimulation were consistent with the previous report (*27*). Hypotonic stimulation applied in combination with 2-LG enhanced $Ca^{2+}{}_i$ (Fig. 6D) to greater extent than 2-LG or hypotonic stimulation alone (Fig. 6E). In contrast, when we stimulated ommatidia with a combination of 2-LG and a hypertonic solution (~416 mOsm), we observed a transient decrease of the 2-LG-evoked response (Fig. 6F). A decrease in pH has been reported to contribute to the activation of TRP and TRPL (*23*). However, we were unable to perform similar experiments using 2-LG and low pH because GCaMP6 is pH-sensitive.

DISCUSSION

Activation of PLC following light stimulation is critical for opening the TRP and TRPL channels in photoreceptor cells. However, many lipids could potentially be generated following stimulation of PLC. To identify candidate lipids that modulate these TRPC channels in vivo, we set out to identify lipids that increase in response to light. Because phototransduction depends on the PLC encoded by *norpA*, we designed the analysis to find lipids that increased upon light stimulation in wild-type flies but in not in the *norpA*

mutant. We found that wild-type but not *norpA* mutant flies exhibited light-dependent increases in the endocannabinoids 2-LG, LEA and phospho-LEA as well as a smaller, statistically insignificant increase in NAG (LinGly). We also found that 2-LG, LEA and LinGly activated TRPC channels in vitro and in isolated ommatidia. The results suggest that one or more of these lipids activates the TRP and TRPL channels in photoreceptor cells (Fig. 7).

We suggest that the endocannabinoid 2-LG is the relevant lipid that activates the TRPC channels in vivo for multiple reasons. 2-LG is generated at levels that are ~60—100-fold higher than LEA, phospho-LEA or LinGly. In addition, the light-dependent rise in 2-LG had greater statistical significance than LEA and phospho-LEA (Fig. 1, C, E and F). Moreover, the statistical significance of the light-induced increase in LEA depended on the one outlier. In contrast to the highly statistically significant light-dependent rise in 2-LG in control flies, the levels of 2-LG in either dark or light exposed $norpA^{P24}$ heads were virtually identical to control heads maintained in the dark. We also observed that the generation of 2-LG relied on *inaE*, which encodes a DAG lipase (*38*). Furthermore, $inaE^{N125}$ flies exhibit a transient ERG response during continuous white light (*38*), supporting the functional importance of *inaE* and its product, 2-LG, for light-stimulated activity of the TRP and TRPL channels. It is noteworthy that 2-LG was reduced after blue light stimulation followed by dark for 30 seconds. This suggests that 2-LG is continuously metabolized during the prolonged depolarizing afterpotential (PDA) when phototransduction continues. We suggest that production of 2-LG, which depends on

INAE, might contribute to the PDA since the PDA is not sustained in *inaE*^{N125} flies after cessation of a blue light stimulation (*38*).

Due to technical challenges in collecting large number of dissected compounds eyes following light stimulation, we performed the lipid analyses on whole heads. Thus, the local, light-dependent rise in 2-LG in the rhabdomeres of the photoreceptor cells is likely to be far greater than the ~30% detected in whole heads. The retina represents ~20% of the mass of the heads, and only eight out of 20 of the retinal cells in each ommatidium are photoreceptor cells. Given that at most 10% of the mass of the heads are rhabdomeres, there might be a >300% increase of 2-LG locally in the rhabdomeres. Thus, we suggest that light causes a sufficient rise in 2-LG in the rhabdomeres to activate TRPC channels. Although a DAG analog has been reported to stimulate the rhabdomeric TRP and TRPL channels (*25*), we did not observe a DAG-induced $Ca^{2+}{}_i$ increase in TRPL-expressing S2 cells. The TRPC channels in the rhabdomeres are activated within 20 milliseconds (*52*), and our lipid analysis was performed following 5 minutes of illumination. Although it is technically more challenging to perform the analysis on second or subsecond timescales, we nevertheless observed a tendency that was not statistically significant for 2-LG to increase upon 10 seconds of light exposure.

Several studies found that LA and other PUFAs can activate TRPC channels (*26, 28, 29*). We also found that LA activated TRPC channels. However, PUFAs including LA are reported to remain unchanged upon illumination (*25*). This is consistent with our lipid analysis indicating that the modest rise in LA in light stimulated animals is not

significant. Although the amounts of LEA and phospho-LEA also rise in a light-dependent manner and are effective at activating the TRPC channels, the findings that the light-dependent increases are much lower than 2-LG suggests that they are not likely to be the prime lipids that activate the highly abundant TRP and TRPL channels in photoreceptor cells. We suggest that the anandamide-related lipid (LEA) and its precursor (phospho-LEA) do not function primarily in activating TRP and TRPL, but rather in some other light-dependent function in photoreceptor cells. One possibility is that these lipids might regulate synaptic vesicle recycling in photoreceptor cells, because this dynamic process depends on proper lipid content at the synapse (*53*). Moreover, feeding flies a diet deficient in PUFAs causes a deficit in the on- and off-transient responses in the electroretinogram, which reflects a decrease in signal transmission from photoreceptor cells to their postsynaptic partners (*54*). Although the increases in LEA and phospho-LEA amounts are PLC- and DAGL-dependent, it is unclear how these lipids are produced in *Drosophila*.

Our results indicated that the specific fatty acid conjugate and the degree of saturation of the fatty acid in the lipid were factors that contributed to the activation of TRP and TRPL. The lipids that increased in a light- and NORPA-dependent manner are conjugated to the PUFA, linoleic acid (C18:2). In contrast, the levels of two other 2-MAGs analyzed that included either a saturated fatty (palmitic acid, C16:0) or a monounsaturated fatty acid (oleic acid, C18:1) were not increased by light. Moreover, oleic acid was ineffective at activated TRPL in vitro or in increasing Ca^{2+} responses in ommatidia. Therefore, we suggest that the action of 2-LG is due to activation of TRPL rather than a non-specific effect of lipids on the properties of the membrane.

Although 2-LG stimulation induced a statistically significant increase in Ca^{2+}_i in *norpA*^{P24} ommatidia compared with *norpA*^{P24};*trpl*^{302};*trp*^{343} ommatidia, the 2-LG-induced Ca^{2+} influx was not eliminated. Although there was remaining Ca^{2+} influx in the mutant lacking TRPL and TRP, there was also a comparable 2-LG-induced Ca^{2+} increase in wild-type ommatidia bathed with the TRP/TRPL channel inhibitor ruthenium red. Therefore, the Ca^{2+} increase in the *norpA*^{P24};*trpl*^{302};*trp*^{343} mutant might be due to a nonspecific effect caused by damage to the ommatidia during dissociation. It is also possible that 2-LG modulates the Na^+/Ca^{2+} exchanger (CalX), which can run in reverse in fly photoreceptor cells (*55*), or voltage-gated channels (*56*).

We found that 2-LG stimulated Ca^{2+} increase with a latency around 30 seconds, which is much slower than the ~20 millisecond response of photoreceptor cells to light (*52*). This large kinetic difference may be a consequence of the need for the colloidal 2-LG particles in the bath solution to be incorporated into the rhabdomeric membrane, then dispersed to reach the channels. The lipid might also need to be flipped into the inner leaflet to act on the channels. We suggest that these events require ~30 seconds. Our data also support the proposal that the action of 2-LG in S2 cells is due to activation of TRPL rather than a non-specific effect of lipids on the plasma membrane, because we did not observe similar increases in Ca^{2+}_i by other unsaturated fatty acid such as OA. The idea that 2-LG is a direct activator of TRPC channels is further strengthened by our finding that 2-LG could activate mammalian TRPC channels.

An open question concerns the mechanism through which 2-LG activates the channels. We propose that 2-LG directly activates TRP and TRPL in vivo because there

are no *Drosophila* homologs of the mammalian endocannabinoid GPCRs CB1 and CB2 (*30, 31*). Moreover, at least six mammalian TRP channels are activated in vitro by cannabinoids and endocannabinoids, including four TRPV channels, TRPA1, and TRPM8 (*57, 58*). An interaction between rat TRPV2 and cannabidiol was identified in a cryo-EM structure (*59*) and differences in the putative binding sites among mammalian TRP channels has been modeled and discussed (*60, 61*). Similarly, the *Drosophila* TRPC channels TRP and TRPL may also be receptors for endocannabinoids. Because CB1 and CB2 are not present in *Drosophila* (*31*), we suggest that TRP channels comprise a class of ionotropic cannabinoid receptors conserved from flies to humans.

A previous and intriguing study proposed that TRP and TRPL are mechanically gated following light-induced activation of the phototransduction cascade and stimulation of NORPA (*27*). The concept is that following stimulation of PLC, the headgroup of DAG, which remains in the membrane, is smaller than PIP_2, thereby resulting in a conformational change in the plasma membrane that causes mechanical activation of the channels. We observed that hypotonic stimulation, which could mimic mechanical stimulation of the ommatidia, enhanced the 2-LG-dependent Ca^{2+} response, whereas hypertonic stimulation had a transient inhibitory effect on the Ca^{2+} response. Based on these findings, we suggest a model in which allosteric modulation of TRP and TRPL by 2-LG along with conformational changes in the membrane due to hydrolysis of PIP_2 both contribute to activation of the TRPC channels (Fig. 7).

MATERIALS AND METHODS

Sources of fly stocks and rearing

w^{1118} was used as the wild-type control. The following flies were obtained from the Bloomington Stock Center (stock numbers are indicated): *trp*^{343} (#9046), *trpl*^{302} (#31433). The following stocks were provided by the indicated investigators: *cn*^{1},*trpl*^{302},*bw*^{1};*trp*^{343},*ninaE-GCaMP6f/Tb*^{1} (R. Hardie), *inaE*^{N125} and *norpA*^{P24} (W. Pak), which was outcrossed to *w*^{1118}. The *w*^{1118},*norpA*^{P24} flies were used throughout this work but are referred to as *norpA*^{P24} for brevity. Flies were reared on standard cornmeal-yeast media: 24,900 ml distilled water, 324 g agar (66-103, Genesee scientific), 1,800 g cornmeal (NC0535320, lab scientific), 449 g yeast (ICN90331280, MP Biomedicals), 240 ml Tegosept (30% in ethanol; H5501, Sigma Aldrich), 72 ml propionic acid (81910, Sigma Aldrich), 8.5 ml phosphoric acid (438081, Sigma Aldrich) and 2,400 ml molasses (62-118, Genesee Scientific). Flies were initially raised in vials or bottles containing the media at 25°C in a chamber under 12-hour light/12-hour dark cycle and transferred to 24-hour dark conditions before experiments as indicated below.

Chemicals

The following chemicals were obtained from Cayman Chemical: linoleic acid (#90150), 2-linoleoyl glycerol (#62260), linoleoyl ethanolamide (#90155), linoleoyl glycine (#9000326), oleic acid (#9000326), 1-oleoyl-2-acetyl-*sn*-glycerol (OAG, #62600), 2-arachidonoyl glycerol (#62160), 2-arachidonoyl glycerol ether (#62165), R-1 methanandamide (#90070), JZL 184 (#13158) and IDFP (#10215). The chemicals were

dissolved in ethanol or DMSO and kept at -80°C. Riluzole [2-Amino-6-(trifluoromethoxy)benzothiazole] (329-92191, FUJIFILM Wako Chemicals) and GSK1702934A (SML2323, Sigma-Aldrich) were dissolved in DMSO and kept at -20°C. Ruthenium red (R2751, Sigma-Aldrich) was dissolved in water and stored at -20°C.

Exposing flies to light and collecting fly heads for lipid analyses

Bottles containing flies were transferred to and maintained in the dark for 7 days after egg laying and handled under a dim red photographic safety light throughout the experiments. ~150 flies (0—4 days old) were collected and transferred into bottles containing fly food. The bottles were wrapped with aluminum foil and placed in the dark. After two days, flies were starved in the dark by transferring the flies into bottles containing 1% agarose, wrapped with aluminum foil and placed in the dark. After 15—17 hours, the flies were anesthetized with CO_2 and transferred into 50 mL tubes (352070, BD Falcon). After 1—2 minutes when the flies began to move, we plugged each tube with a cotton ball, which we pushed down to the 10-mL line. The tubes were covered with aluminum foil and placed in a rack for 10 minutes to allow the flies to continue to recover from the CO_2 exposure. After removing the aluminum foil, we left the cotton ball in each tube and secured the top of each tube with a screw cap. We then placed the tubes in a 37°C incubator for 3 minutes since PLC activity is higher at 37°C than at the standard incubation temperature of 25°C (*20*).

To enable us to compare lipids that increase upon light exposure, we either maintained the tubes with the flies in the dark or exposed the flies to blue light from the

side of the tube (~0.3—1.0 mW at the distal and the proximal sides of the tube, respectively) for 5 minutes. In some experiments, flies were further stimulated with orange light from the side of the tube (~1.1—1.5 mW at the distal and the proximal sides of the tube, respectively) for 1 minute. The tubes were immediately immersed in liquid nitrogen for 30 seconds. To mechanically separate the head and bodies, we removed the cotton plugs, reinserted the screw caps, and vigorously vortexed the tubes. The frozen samples were then passed through 25 and 40 mesh sieves. The fly heads, which were trapped on the 40 mesh sieves, were quickly transferred into chilled 1.5 ml black microfuge tubes (T7100BK, Argos technologies) and stored at -80°C until we performed the lipid extractions.

Lipid extraction from fly heads

500 μL of methanol was added to each tube containing 4—8 mg of fly heads followed by 100 pmols, deuterium-labeled *N*-arachidonoyl glycine (d8NAGly), to act as an internal standard. The tubes were then closed, vortexed for 30 seconds and left in darkness on ice for 1 hour, vortexed again for 30 seconds and left to process for another hour in darkness on ice. The samples were then centrifuged at 19,000xg at 24°C for 20 minutes. The supernatants were collected and placed in polypropylene tubes (15 ml) and 1.5 ml of HPLC-grade water was added making the final supernatant/water solution 25% organic. A partial purification of lipids was achieved using a preppy apparatus assembled with 500 mg C18 solid-phase extraction columns. The columns were conditioned with 5 mL of HPLC-grade methanol immediately

followed by 2.5 mL of HPLC-grade water under pressure. The supernatant/water solution was then loaded onto the C18 column and washed with 2.5 mL of HPLC grade water followed by 1.5 mL of 40% methanol. Elutions of 1.5 mL of 60%, 70%, 85% and 100% methanol were collected in individual autosampler vials and then stored in a -80°C freezer until mass spectrometer analysis.

LC/MS/MS analysis and quantification

Samples were removed from the -80°C freezer and allowed to warm to room temperature then vortexed for approximately 1 minute before being placed into the autosampler and held at 24°C (Agilent 1100 series autosampler, Palo Alto, CA) for the LC/MS/MS analysis. 20 μL of eluants were injected separately to be rapidly separated using a C18 Zorbax reversed-phase analytical column to scan for individual compounds. Gradient elution (200 μL/min) then occurred, under the pressure created by two Shimadzu 10AdVP pumps (Columbia, MD). Next, electrospray ionization was done using an Applied Biosystems/MDS SCIEX (Foster City, CA) API3000 triple quadrupole mass spectrometer. All compounds were analyzed using multiple reaction monitoring (MRM). Synthetic standards were used to generate optimized MRM methods and standard curves for analysis. We reported the MRM parent/fragment pairs previously (*33*), with the exception of phospho-LEA, which is MRM[-] 403.5/58.5. The mobile phases are also the same as we reported previously (*33*): mobile phase A, 80% HPLC-grade H_2O/20% HPLC-grade methanol, 1 mM ammonium acetate; mobile phase B,

100% HPLC-grade methanol, 1 mM ammonium acetate. Extreme outliers (10 times or higher than the average value in a group) were omitted from the analyses.

Ca^{2+} imaging

Schneider 2 (S2) cells carrying a *trpl-egfp* transgene (gift from B. Minke) (*40*) were grown in 60 mm dishes (353002, Falcon) at 25°C in 4 mL Schneider's media (21720-024, Gibco) that contained 10% inactivated fetal bovine serum (10437-028, Gibco) and 50 mg/mL penicillin/50 units/mL streptomycin (15140-122, Gibco). S2 cells were seeded on 8 mm round cover glasses (Matsunami) in a 35 mm dishes (1000-035, Iwaki). We then added 2 μL 500 mM $CuSO_4$ (039-04412, Wako) to 2 mL culture medium (final 500 μM) and incubated the cells for 24 hours in a 25°C incubator to induce expression of the gene encoding TRPL::EGFP. The cells without the $CuSO_4$ treatment were used as the control cells that did not express TRPL. To load the cells with Fura-2 AM, we added 1 mL of the following mixture to the culture media and incubated the cells at 25°C incubator for 1—3 hours: 5 μM Fura-2 AM (F-1201, Life Technologies), 250 μM probenecid (162-26112, Wako), 20% pluronic F-127 (P2443, Sigma). The cells were then allowed to recover for 15 minutes in a bath solution containing 130 mM NaCl, 5 mM KCl, 2 mM $MgCl_2$, 2 mM $CaCl_2$, 30 mM sucrose, and 10 mM N-Tris(hydroxymethyl)methyl-2-aminoethanesulfonic acid (TES), after adjusting the pH to 7.2 with NaOH. The cover glasses were mounted in a chamber (RC-26G; Warner Instruments) connected to a gravity flow system to deliver various stimuli. A xenon lamp was used as an illumination source. To obtain fluorescent intensities of Ca^{2+}-bound and

Ca^{2+}-free Fura-2, we excited the cells at 340 and 380 nm, respectively, and emission was monitored at 510 nm with a sCMOS camera (Zyla 4.2 Plus; Andor Technology) used with a fluorescent microscope (Eclipse TE2000-U, Nikon). The data were acquired using iQ2 software (Andor Technology) and the ratio values (340/380) were calculated with Fiji software (*62*). Cells showing a lower response with ionomycin than with lipid stimulation were omitted from the quantification.

To evaluate the effect of 2-LG on activation of mouse TRPC5 and TRPC6, we expressed these channels in human embryonic kidney 293T (HEK293T) cells. The cells were cultured in Dulbecco's modified Eagle Medium (044-29765, Wako) supplemented with 10% heat-inactivated fetal bovine serum (10437-028, Gibco), 50 mg/mL penicillin/50 units/mL streptomycin (15140-122, Gibco) and 2 mM GlutaMAX (35050-061, Gibco). The HEK293 cells were transiently transfected with 1 μg of mouse TRPC5/pCI-neo or TRPC6/pCI-neo (gifts from Dr. Yasuo Mori) and 0.1 μg pCMV-DsRed using Lipofectamine reagent (18324-020, Invitrogen) and Plus reagent (11514-015, Invitrogen) dissolved in 1X OPTI-MEM medium (31985-070, Thermo Fisher). After incubation for 3–4 h, the HEK293 cells were reseeded onto 12-mm coverslips (Matsunami) in a 35 mm dishes (1000-035, Iwaki) and further incubated for 24—48 hours at 33°C (TRPC5) or 37°C (TRPC6) in 5% CO_2. To load the cells with Fura-2 AM, we added 1 mL of the culture media containing 5 μM Fura-2 AM (F-1201, Life Technologies) and incubated the cells at 33°C (TRPC5) or 37°C (TRPC6) for 1–2 hours. The extracellular solution contained 140 mM NaCl, 5 mM KCl, 2 mM $MgCl_2$, 2 mM $CaCl_2$, 10 mM HEPES and 10 mM glucose at pH 7.4. The cover glasses were mounted

in a chamber (RC-26G; Warner Instruments) connected to a gravity flow system to deliver the various stimuli. Riluzole was kept at a temperature slightly cooler than room temperature (15–20°C) to enhance the responsiveness of TRPC5, which is cold-sensitive (*63*). We followed changes in Fura-2 fluorescence as described above. DsRed-expressing cells were chosen for determining the changes in the fluorescence ratio, and cells showing no response to riluzole or GSK1702934A (ratio increase less than 0.1) were omitted from the quantification.

We obtained an average trace for each sample and calculated the change in Ca^{2+}_i as follows: Ca^{2+}_i response=$(F_{res} – F_{min})/(F_{max} – F_{min})$. To normalize the responses, we subtracted the minimum values during the basal period (F_{min}) from the responses every 3 sec (F_{res}). We also subtracted the F_{min} from the maximum value obtained due to addition of the ionomycin (F_{max}) (I0634, Sigma). After the normalization we extracted the maximum increase in Ca^{2+}_i (Ca^{2+}_i max) during the stimulation period for further analysis. During stimulation with 2-AG ether, we observed non-specific Ca^{2+}_i responses, which we recognized due to stochastic and sudden ratio increases in $CuSO_4$-induced (TRPL-expressing) and non-induced control cells. Traces containing these non-specific responses were omitted from the analyses.

Dissociation of ommatidia

All ommatidia were isolated from *norpA*^{P24} flies to prevent light-induced activation of the TRP and TRPL channels. The flies were maintained under standard light/dark cycles and transferred to a constant darkness after initiating new crosses to eliminate

any possibility of light-induced retinal degeneration. Male progeny were selected for the experiments with isolated ommatidia because *norpA* is on the X chromosome, thereby simplifying the crosses needed to obtain flies with the $norpA^{P24}$ mutation, which is recessive. The $trpl^{302}$ (*10*) and $trpl^{343}$ (*64*) mutations are recessive. The control flies were heterozygous for $trpl^{302}$ and $trpl^{343}$ ($norpA^{P24}/Y$;cn^{1},$trpl^{302}$,$bw^{1}/+$;trp^{343},*ninaE-GCaMP6f/+*) and were obtained by crossing $norpA^{P24}$ females and cn^{1},$trpl^{302}$,bw^{1};trp^{343},*ninaE-GCaMP6f*/Tb^{1} males. The trp^{343} mutant was also heterozygous for $trpl^{302}$ ($norpA^{P24}/Y$;cn^{1},$trpl^{302}$,$bw^{1}/+$;trp^{343},*ninaE-GCaMP6f*/trp^{343}) and was obtained by crossing $norpA^{P24}$;+;trp^{343} females and cn^{1},$trpl^{302}$,bw^{1};trp^{343},*ninaE-GCaMP6f*/Tb^{1} males. The $trpl^{302}$ mutant was also heterozygous for trp^{343} ($norpA^{P24}/Y$;*cn1*,$trpl^{302}$,bw^{1};trp^{343},*ninaE-GCaMP6f/+*) and was obtained by crossing $norpA^{P24}$;$trpl^{302}$ females and cn^{1},$trpl^{302}$,bw^{1};trp^{343},*ninaE-GCaMP6f*/Tb^{1} males. The $trpl^{302}$;trp^{343} mutant ($norpA^{P24}/Y$;cn^{1},$trpl^{302}$,bw^{1};trp^{343},*ninaE-GCaMP6f*/trp^{343}) was obtained by crossing $norpA^{P24}$;$trpl^{302}$;trp^{343} females and cn^{1},$trpl^{302}$,bw^{1};trp^{343},*ninaE-GCaMP6f*/Tb^{1} males.

Dissection of ommatidia was performed similar to that described previously (*65*). Briefly, we performed dissections under a dim LED light source with a red filter (RG610, Schott), which is functionally equivalent to darkness for the flies. To conduct each experiment, two males (within 4 hours of eclosion) were collected using CO_2 and the heads were removed, briefly soaked in 70% ethanol and then immersed in a drop of dissection media containing Schneider's medium and 0.2% bovine serum albumin (fatty acid-free, A8806, Sigma). The four eye cups were dissected using forceps and the

retina were scooped out using a micro scooper made from a minutien pin (26002-10, Fine Science Tools). The retinas were collected using a fire-polished trituration glass pipette made from a glass capillary (outer diameter 1.2 mm, inner diameter 0.69 mm, GC120-10, Warner Instruments) and washed with and incubated in fresh dissection media for 20 minutes in the dark. Surrounding pigmented glia were removed by rapid aspiration/expiration and the retina were transferred to a drop (30 μL) of the dissection media. Ommatidia were then mechanically dissociated by repetitive pipetting using three fire-polished trituration pipettes with different inner diameters until almost all the ommatidia were isolated from the lamina layers. Dissociated ommatidia were immediately used for subsequent imaging experiments and maintained in the drop in a dark for up to 60 minutes.

GCaMP6 imaging

Each ommatidial suspension (8—9 μL) was placed on the glass bottom of a chamber (RC-26G; Warner Instruments), and the ommatidia were allowed to settle down to the bottom for 3—4 minutes. To wash out floating cells and the dissection media, the chamber was filled and perfused with an extracellular solution containing 120 mM NaCl, 5 mM KCl, 4 mM $MgCl_2$, 1.5 mM $CaCl_2$, 25 mM L-proline, 5 mM L-alanine, and 10 mM TES, which was adjusted to pH 7.15 with NaOH. The Ca^{2+}-free experiments were performed with a solution that was nominally Ca^{2+}-free by omitting 1.5 mM $CaCl_2$ from the extracellular solution. To test the effect of ruthenium red (RuR), the ommatidia were treated with 30 μM 2-LG in the presence of 10 μM RuR for 2 minutes, followed by

30 μM 2-LG alone for 3 minutes. To examine the impact of hypotonic or hypertonic conditions on channel activation by 2-LG, the chamber was perfused with basal isotonic solution containing 75 mM NaCl, 5 mM KCl, 4 mM $MgCl_2$, 1.5 mM $CaCl_2$, 25 mM L-proline, 5 mM L-alanine, and 10 mM TES, 100 mM sucrose, which was adjusted to pH 7.15 with NaOH (316.5 mOsm). The ommatidia were stimulated with hypotonic solution (isotonic solution without sucrose: 216.5 mOsm) or hypertonic solution (isotonic solution supplemented with 100 mM sucrose: 416.5 mOsm) in the presence or absence of 30 μM 2-LG. A xenon lamp was used as an illumination source.

To monitor the fluorescent intensity of the GCaMP6f, the ommatidia were excited with 472 nm light and emissions were monitored at 520 nm with a sCMOS camera (Zyla 4.2 Plus; Andor Technology) attached to a fluorescent microscope (Eclipse TE2000-U, Nikon). To minimize photobleaching of GCaMP6f and an exhaustion of cells caused by light activation of the rhodopsins, we excited the ommatidia every 6 seconds for 60 or 90 milliseconds. Ionomycin (5 μM) was applied in the end of protocol to evaluate the viability of ommatidia.

Data were acquired with iQ2 software (Andor Technology) and the fluorescent intensities were calculated with Fiji software (*62*). A region of interest (ROI) was defined as the distal half (the outer side) of the ommatidia since $Ca^{2+}{}_i$ responses were relatively higher in this region (Fig. 4, A and B) and the proximal half (the inner side) of ommatidia was prone to vibration during the perfusion. Typically, 15—30 ommatidia in a field was chosen for analysis and cells with obvious damage or small responses to ionomycin or were out of focus were omitted from the analysis. Changes in fluorescence intensity

($\Delta F/F_0$) was used to assess the $Ca^{2+}{}_i$ responses [$(F_t - F_{basal})/F_{basal}$]. F_t corresponds to the value obtained every 6 seconds. F_{basal} is the average during the first 1 minute (0.1% EtOH alone) in every ommatidium. The background values were measured in *norpA*^{P24} ommatidia that do not express GCaMP6f in the presence of 0.1% EtOH. The average background values were subtracted from the fluorescent intensities in all samples. The maximum response (max $\Delta F/F_0$) with each lipid (in 0.1% EtOH) was obtained during the 4-minute stimulation period (60—300 seconds) after addition of the lipids. The areas under the curve during the stimulation period (60—300 seconds after addition of the lipids) were calculated using a trapezoidal rule [$(F_t+F_{t+1})/2$ x 6 (sampling interval)]. For no or low responding ommatidia, the number of cells having max $\Delta F/F_0 \leq 0.2$ were counted and divided by the total number of cells in each sample to obtain the proportion. Cells showing a lower response with ionomycin than with lipid stimulation were omitted from the quantification.

Quantification and statistical analysis

The data are represented as means ± SEMs. The number of times each experiment was performed (n) is indicated in the figure legends. We used the unpaired, two-tailed Student's *t*-test to determine the statistical significance of two samples that had an equal variance and a normal distribution. If any of the two sets of data was not normally distributed, we performed the Mann-Whitney U test. To determine the statistical significance of the data using ommatidia in Ca^{2+}-free versus Ca^{2+}-containing bath conditions, and the data using ommatidia in RuR-treated versus RuR-removed

conditions, we used the paired, two-tailed Student's *t*-test. To evaluate the statistical significance of multiple samples that had an equal variance and a normal distribution, we used one-way ANOVA with the Dunnett's *post hoc* analysis. If any of the multiple sets of data was not normally distributed, we used the Kruskal-Wallis test followed by the Steel test or the Steel-Dwass test. To evaluate the statistical significance of multiple samples in the no or low response populations, we used one-way ANOVA with the Tukey's *post hoc* analysis. Statistical tests were performed using Prism 7 (Graphpad) or JMP 14.2 (SAS Institute). Asterisks indicate statistical significance, where *$p < 0.05$, **$p < 0.01$ and ***$p < 0.001$.

Supplementary Materials

Fig. S1-S5.

Data File S1.

References and Notes:

1. K. W. Yau, R. C. Hardie, Phototransduction motifs and variations. *Cell* **139**, 246-264 (2009).
2. C. Montell, *Drosophila* visual transduction. *Trends Neurosci.* **35**, 356-363 (2012).
3. C. Montell, *Drosophila* sensory receptors—a set of molecular Swiss Army Knives. *Genetics* **217**, 1-34 (2021).

4. W. L. Pak, J. Grossfield, K. S. Arnold, Mutants of the visual pathway of *Drosophila melanogaster*. *Nature* **227**, 518-520 (1970).

5. R. C. Hardie, M. Juusola, Phototransduction in *Drosophila*. *Curr. Opin. Neurobiol.* **34C**, 37-45 (2015).

6. B. T. Bloomquist *et al.*, Isolation of a putative phospholipase C gene of Drosophila, *norpA*, and its role in phototransduction. *Cell* **54**, 723-733 (1988).

7. C. Montell, G. M. Rubin, Molecular characterization of the Drosophila *trp* locus: a putative integral membrane protein required for phototransduction. *Neuron* **2**, 1313-1323 (1989).

8. R. C. Hardie, B. Minke, The *trp* gene is essential for a light-activated Ca^{2+} channel in Drosophila photoreceptors. *Neuron* **8**, 643-651 (1992).

9. A. M. Phillips, A. Bull, L. E. Kelly, Identification of a Drosophila gene encoding a calmodulin-binding protein with homology to the *trp* phototransduction gene. *Neuron* **8**, 631-642 (1992).

10. B. A. Niemeyer, E. Suzuki, K. Scott, K. Jalink, C. S. Zuker, The Drosophila light-activated conductance is composed of the two channels TRP and TRPL. *Cell* **85**, 651-659 (1996).

11. C. Montell *et al.*, A unified nomenclature for the superfamily of TRP cation channels. *Mol. Cell* **9**, 229-231 (2002).

12. P. D. Wes *et al.*, TRPC1, a human homolog of a *Drosophila* store-operated channel. *Proc. Natl. Acad. Sci. USA* **92**, 9652-9656 (1995).

13. X. Zhu, P. B. Chu, M. Peyton , L. Birnbaumer, Molecular cloning of a widely expressed human homologue for the *Drosophila trp* gene. *FEBS Lett.* **373**, 193-198 (1995).

14. L. Liu, K. R. MacKenzie, N. Putluri, M. Maletic-Savatic, H. J. Bellen, The glia-neuron lactate shuttle and elevated ROS promote lipid synthesis in neurons and lipid droplet accumulation in glia via APOE/D. *Cell Metab.* **26**, 719-737 e716 (2017).

15. G. Lin *et al.*, Phospholipase *PLA2G6*, a Parkinsonism-associated gene, affects Vps26 and Vps35, retromer function, and ceramide levels, similar to α-synuclein gain *Cell Metab.* **28**, 605-618 e606 (2018).

16. L. McGurk, A. Berson, N. M. Bonini, *Drosophila* as an *in vivo* model for human neurodegenerative disease. *Genetics* **201**, 377-402 (2015).

17. J. M. Warrick *et al.*, Expanded polyglutamine protein forms nuclear inclusions and causes neural degeneration in *Drosophila*. *Cell* **93**, 939-949 (1998).

18. W. L. Pak, in *Molecular genetics of inherited eye disorders,* A. F. Wright, B. Jay, Eds. (Harwood Academic Publishers, Chur, Switzerland, 1994), pp. 29-52.

19. N. Zhuang, L. Li, S. Chen, T. Wang, PINK1-dependent phosphorylation of PINK1 and Parkin is essential for mitochondrial quality control. *Cell Death Dis.* **7**, e2501 (2016).

20. F. D. Huang, H. J. Matthies, S. D. Speese, M. A. Smith, K. Broadie, Rolling blackout, a newly identified PIP_2-DAG pathway lipase required for *Drosophila* phototransduction. *Nat. Neurosci.* **7**, 1070-1078 (2004).

21. P. Raghu *et al.*, Constitutive activity of the light-sensitive channels TRP and TRPL in the *Drosophila* diacylglycerol kinase mutant, *rdgA*. *Neuron* **26**, 169-179 (2000).

22. J. K. Acharya, K. Jalink, R. W. Hardy, V. Hartenstein, C. S. Zuker, $InsP_3$ receptor essential for growth and differentiation but not for vision in Drosophila. *Neuron* **18**, 881-887 (1997).

23. J. Huang *et al.*, Activation of TRP channels by protons and phosphoinositide depletion in *Drosophila* photoreceptors. *Curr. Biol.* **20**, 189-197 (2010).

24. R. Delgado *et al.*, Light-induced opening of the TRP channel in isolated membrane patches excised from photosensitive microvilli from *Drosophila* photoreceptors. *Neuroscience* **396**, 66-72 (2019).

25. R. Delgado, Y. Muñoz, H. Peña-Cortés, P. Giavalisco, J. Bacigalupo, Diacylglycerol activates the light-dependent channel TRP in the photosensitive microvilli of *Drosophila melanogaster* photoreceptors. *J. Neurosci.* **34**, 6679-6686 (2014).

26. R. Delgado, J. Bacigalupo, Unitary recordings of TRP and TRPL channels from isolated Drosophila retinal photoreceptor rhabdomeres: activation by light and lipids. *J. Neurophysiol.* **101**, 2372-2379 (2009).

27. R. C. Hardie, K. Franze, Photomechanical responses in *Drosophila* photoreceptors. *Science* **338**, 260-263 (2012).

28. S. Chyb, P. Raghu, R. C. Hardie, Polyunsaturated fatty acids activate the Drosophila light-sensitive channels TRP and TRPL. *Nature* **397**, 255-259 (1999).

29. S. Lev, B. Katz, V. Tzarfaty, B. Minke, Signal-dependent hydrolysis of phosphatidylinositol 4,5-bisphosphate without activation of phospholipase C: Implications on gating of *Drosophila* TRPL (Transient Receptor Potential-Like) channel. *J. Biol. Chem.* **287**, 1436–1447 (2012).

30. A. M. Gregus, M. W. Buczynski, Druggable targets in endocannabinoid signaling. *Advances in experimental medicine and biology* **1274**, 177-201 (2020).

31. J. McPartland, V. Di Marzo, L. De Petrocellis, A. Mercer, M. Glass, Cannabinoid receptors are absent in insects. *J. Comp. Neurol.* **436**, 423-429 (2001).

32. S. G. Britt, R. Feiler, K. Kirschfeld, C. S. Zuker, Spectral tuning of rhodopsin and metarhodopsin in vivo. *Neuron* **11**, 29-39 (1993).

33. G. Tortoriello *et al.*, Targeted lipidomics in *Drosophila melanogaster* identifies novel 2-monoacylglycerols and *N*-acyl amides. *PLoS One* **8**, e67865 (2013).

34. G. Tortoriello *et al.*, Genetic manipulation of sn-1-diacylglycerol lipase and CB_1 cannabinoid receptor gain-of-function uncover neuronal 2-linoleoyl glycerol signaling in *Drosophila melanogaster*. *Cannabis Cannabinoid Res.* **6**, 119-136 (2021).

35. T. Yoshioka *et al.*, Evidence that arachidonic acid is deficient in phosphatidylinositol of *Drosophila* heads. *J. Biochem.* **98**, 657-662 (1985).

36. L. R. Shen *et al.*, *Drosophila* lacks C20 and C22 PUFAs. *J. Lipid Res.* **51**, 2985-2992 (2010).

37. J. Liu *et al.*, A biosynthetic pathway for anandamide. *Proc. Natl. Acad. Sci. USA* **103**, 13345-13350 (2006).

38. H. T. Leung *et al.*, DAG lipase activity is necessary for TRP channel regulation in *Drosophila* photoreceptors. *Neuron* **58**, 884–896 (2008).

39. T. Wang, C. Montell, Phototransduction and retinal degeneration in *Drosophila*. *Pflugers Arch.* **454**, 821-847 (2007).

40. M. Parnas, B. Katz, B. Minke, Open channel block by Ca^{2+} underlies the voltage dependence of *Drosophila* TRPL channel. *J. Gen. Physiol.* **129**, 17-28 (2007).

41. J. Z. Long *et al.*, Selective blockade of 2-arachidonoylglycerol hydrolysis produces cannabinoid behavioral effects. *Nat. Chem. Biol.* **5**, 37-44 (2009).

42. D. K. Nomura *et al.*, Activation of the endocannabinoid system by organophosphorus nerve agents. *Nat. Chem. Biol.* **4**, 373-378 (2008).

43. K. Laine, K. Jarvinen, R. Mechoulam, A. Breuer, T. Jarvinen, Comparison of the enzymatic stability and intraocular pressure effects of 2-arachidonylglycerol and noladin ether, a novel putative endocannabinoid. *Invest. Ophthalmol. Vis. Sci.* **43**, 3216-3222 (2002).

44. V. Abadji *et al.*, (R)-methanandamide: a chiral novel anandamide possessing higher potency and metabolic stability. *J. Med. Chem.* **37**, 1889-1893 (1994).

45. A. P. Albert, Gating mechanisms of canonical transient receptor potential channel proteins: role of phosphoinositols and diacylglycerol. *Advances in experimental medicine and biology* **704**, 391-411 (2011).

46. K. Venkatachalam, C. Montell, TRP channels. *Annu. Rev. Biochem.* **76**, 387-417 (2007).

47. J. M. Richter, M. Schaefer, K. Hill, Riluzole activates TRPC5 channels independently of PLC activity. *Br. J. Pharmacol.* **171**, 158-170 (2014).

48. P. L. Yang *et al.*, GSK1702934A and M085 directly activate TRPC6 via a mechanism of stimulating the extracellular cavity formed by the pore helix and transmembrane helix S6. *J. Biol. Chem.* **297**, 101125 (2021).

49. S. Asteriti, C. H. Liu, R. C. Hardie, Calcium signalling in *Drosophila* photoreceptors measured with GCaMP6f. *Cell Calcium* **65**, 40-51 (2017).

50. B. Minke, C. Wu, W. L. Pak, Induction of photoreceptor voltage noise in the dark in Drosophila mutant. *Nature* **258**, 84-87 (1975).

51. B. Minke, Light-induced reduction in excitation efficiency in the *trp* mutant of Drosophila. *J. Gen. Physiol.* **79**, 361-385 (1982).

52. R. Ranganathan, G. L. Harris, C. F. Stevens, C. S. Zuker, A *Drosophila* mutant defective in extracellular calcium-dependent photoreceptor deactivation and desensitization. *Nature* **354**, 230-232 (1991).

53. E. Marza *et al.*, Polyunsaturated fatty acids influence synaptojanin localization to regulate synaptic vesicle recycling. *Mol. Biol. Cell* **19**, 833-842 (2008).

54. A. B. Ziegler *et al.*, Lack of dietary polyunsaturated fatty acids causes synapse dysfunction in the *Drosophila* visual system. *PLoS One* **10**, e0135353 (2015).

55. T. Wang *et al.*, Light activation, adaptation, and cell survival functions of the Na+/Ca2+ exchanger CalX. *Neuron* **45**, 367-378 (2005).

56. F. Elinder, S. I. Liin, Actions and mechanisms of polyunsaturated fatty acids on voltage-gated ion channels. *Front. Physiol.* **8**, 43 (2017).

57. C. Muller, P. Morales, P. H. Reggio, Cannabinoid ligands targeting TRP channels. *Front. Mol. Neurosci.* **11**, 487 (2019).

58. H. B. Bradshaw, S. Raboune, J. L. Hollis, Opportunistic activation of TRP receptors by endogenous lipids: exploiting lipidomics to understand TRP receptor cellular communication. *Life Sci.* **92**, 404-409 (2013).

59. R. A. Pumroy *et al.*, Molecular mechanism of TRPV2 channel modulation by cannabidiol. *eLife* **8** (2019).

60. C. Muller, P. H. Reggio, An analysis of the putative CBD binding site in the ionotropic cannabinoid receptors. *Front. Cell. Neurosci.* **14**, 615811 (2020).

61. C. Muller, D. L. Lynch, D. P. Hurst, P. H. Reggio, A closer look at anandamide interaction with TRPV1. *Front Mol Biosci* **7**, 144 (2020).

62. J. Schindelin *et al.*, Fiji: an open-source platform for biological-image analysis. *Nat. Methods* **9**, 676-682 (2012).

63. K. Zimmermann *et al.*, Transient receptor potential cation channel, subfamily C, member 5 (TRPC5) is a cold-transducer in the peripheral nervous system. *Proc. Natl. Acad. Sci. USA* **108**, 18114-18119 (2011).

64. T. Wang, Y. Jiao, C. Montell, Dissecting independent channel and scaffolding roles of the *Drosophila* transient receptor potential channel. *J. Cell Biol.* **171**, 685-694 (2005).

65. R. C. Hardie, Whole-cell recordings of the light-induced current in dissociated *Drosophila* photoreceptors - evidence for feedback by calcium permeating the light-sensitive channels. *Proc. Roy. Soc. Lond. B Biol. Sci.* **245**, 203-210 (1991).

Acknowledgments:

We thank Dr. Baruch Minke (Hebrew University) for sharing the *trpl*-expressing stable S2 cells, Dr. Roger Hardie (Cambridge University) for sharing valuable fly stocks and suggestions for the ommatidia dissociation protocol, and Dr Yasuo Mori (Kyoto University) for sharing the mouse TRPC5 and TRPC6 expression vectors. We thank Naomi Fukuta for performing Fura2-imaging of mouse TRPC5 and TRPC6, and Dr. Zijing Chen for collecting fly head samples from *inaE*^{N125} for lipid analyses.

Funding:

The National Institute of Allergy and Infectious Diseases AI169386 (CM)

The National Institute on Drug Addiction DA039463 (HBB)

Grant-in-Aid for Scientific Research from the Ministry of Education, Culture, Sports, Science and Technology in Japan #15H02501 (MT)

Grant-in-Aid for Scientific Research from the Ministry of Education, Culture, Sports, Science and Technology in Japan #17H07337 (TS)

Grant-in-Aid for Scientific Research from the Ministry of Education, Culture, Sports, Science and Technology in Japan #18K06495 (TS).

Author contributions:

Conceptualization: TS, CM

Methodology: TS, HBB, EL, CM

Investigation: TS, HBB, EL, AC

Formal Analysis: TS, HBB, EL

Writing — original Draft: TS, CM

Writing — review and editing: TS, HBB, MT, CM

Funding acquisition: TS, HBB, MT, CM

Supervision: TS, CM

Competing interests:

The authors declare that they have no competing interests.

Data and materials availability:

All data needed to evaluate the conclusions in the paper are present in the paper or the Supplementary Materials.

Figure Legends:

Fig. 1. Relative lipid levels in control (w^{1118}), $norpA^{P24}$ and $inaE^{N125}$ heads from flies maintained in the dark and after light exposure. (A) Schematic of protocol for collecting heads from flies maintained at 37°C in the dark for 8 minutes or from flies kept in the dark for 3 minutes and then exposed to blue light for 5 minutes. “Dark” indicates flies that were processed using a dim photographic safety light right before the 37°C incubation, which is functionally dark to *Drosophila*. After freezing in liquid N_2, and vortexing, the heads were collected over a sieve, lipids were extracted and analyzed by

LC/MS/MS. **(B)** Pathway for production of endocannabinoids and other lipids from phosphatidylinositol 4,5-bisphosphate [PI(4,5)P_2]. DAG, diacylglycerol; 2-LG, 2-linoleoyl glycerol; 2-MAG, 2-monoacylglycerol; LA, linoleic acid. **(C** to **F)** Concentrations (nmoles/gram) of the indicated lipids extracted from control and *norpA*^{P24} heads that were kept in the dark or exposed to blue light: 2-linoleoyl glycerol (2-LG) levels after 5-minute blue light exposure (C), 2-LG levels after 10-second blue light exposure (D), linoleoyl ethanolamide (LEA) levels after 5-min blue light exposure (E), and phospho-linoleoyl ethanolamide (phospho-LEA) levels after 5-min blue light exposure (F). The lipid metabolites in (C), (E) and (F) were analyzed from the same set of samples. Data are presented as means ± SEMs (n=12 independent experiments; ~1,800 fly heads per group). *$p < 0.05$, **$p < 0.01$ (Mann-Whitney U test). **(G)** Concentrations (nmoles/gram) of 2-LG extracted from *inaE*^{N125} heads that were kept in the dark or exposed to blue light for 5 minutes. The control maintained in dark was used for comparison. The difference in the concentration of 2-LG from (C) is due to modifications in the LC/MS/MS system. Data are presented as means ± SEMs (n=12 independent experiments; ~1,800 fly heads per group). ***$p < 0.001$ (Steel test).

Fig. 2. Effects of endocannabinoids and *N*-acyl glycine on TRPL-dependent changes in Fura-2 ratio in S2 cells. (A) Comparison of the maximum increase in intracellular Ca^{2+} (Ca^{2+}_i) in response to the indicated lipids. Lipids were added at 100 μM, except for 300 μM oleic acid (OA). The Cu^{2+} (-) cells did not express TRPL and the Cu^{2+} (+) cells expressed TRPL. Data are presented as means ± SEMs (n=3—6

independent experiments; ~300—600 cells per group). **(B** to **F)** Fura-2 dose responses of TRPL-expressing cells to 2-LG (B) and representative traces in response to 2-LG (C). Values in (B) were normalized to ionomycin (Iono). Fura-2 dose responses to 2-LG, LEA, LinGly and LA (D). Representative traces in response to 100 μM LEA (E) and to 100 μM LinGly (F) are shown. The data are the maximum $Ca^{2+}{}_i$ during the stimulation period (60—360 seconds after lipid addition). Basal values were subtracted, and percentages were normalized to the maximum values obtained with 5 μM Iono. Curves were fitted using nonlinear regression with variable slopes. The red and black bars (B, C, E and F) indicate the perfusion of the lipids and Iono, respectively. Data are presented as means ± SEMs (n=5—7 independent experiments; ~500—700 cells per group).

Fig. 3. Effects of lipase inhibitors and combination of lipids on Fura-2 responses in TRPL-expressing S2 cells. (A) The effects of a monoacyl glycerol lipase (MAGL) inhibitor (JZL 184, 80 nM) or a MAGL/fatty acid amide hydrolase inhibitor (IDFP, 30 nM) on increases in $Ca^{2+}{}_i$ induced by 2-LG (10 μM), LEA (10 μM) and LinGly (10 μM). Cells were pretreated with inhibitor or vehicle (0.1% dimethyl sulfoxide) one minute before lipid application. Background $Ca^{2+}{}_i$ were obtained in non-induced Cu^{2+} (-) cells with the vehicle alone, 80 nM JZL 184 or 30 nM IDFP. Values were normalized to the maximum values obtained with 5 μM Iono. Data are presented as means ± SEMs (n=3 independent experiments for TRPL-expressing cells, n=4—5 independent experiments for cells not expressing TRPL. ~300—500 cells per group). **(B—D)** The effect of mixing

2-LG, LEA, LinGly and linoleic acid (LA) on increases in Ca^{2+}_i in TRPL-expressing cells. The numbers indicate the concentration of lipids (μM). Data are presented as means ± SEMs (n=3—4 independent experiments; ~300—400 cells per group).

Fig. 4. Effect of 2-LG on mammalian TRPC5 and TRPC6 expressed in HEK293 cells. (A,B) Representative Fura-2 responses to 2-LG in cells expressing mouse TRPC5 (A) or cells transfected with the empty vector (B). HEK293 cells were stimulated with 100 μM 2-LG by perfusion, then with 100 μM riluzole to check for channel function. The red and purple bars indicate the perfusion of 2-LG and riluzole, respectively. Cell viability was confirmed by applying 5 μM ionomycin (Iono, black bar). **(C)** Quantification of the maximum increase in intracellular Ca^{2+} (Ca^{2+}_i) in response to 2-LG in TRPC5-expressing cells or vector-transfected cells. **(D,E)** Representative Fura-2 responses to 2-LG in mouse TRPC6-expressing cells (D) and vector-transfected cells (E). HEK293 cells were stimulated with 100 μM 2-LG by perfusion, then with 100 μM GSK1702934A (GSK) to check for channel function. The red and blue bars indicate the perfusion of 2-LG and GSK1702934A, respectively. Cell viability was confirmed by applying 5 μM ionomycin (Iono, black bar). **(F)** Quantification of the maximum increase in intracellular Ca^{2+} (Ca^{2+}_i) in response to 2-LG in TRPC6-expressing cells or vector-transfected cells. The data in (C) and (F) are the maximum Ca^{2+}_i during the stimulation period (60—360 seconds after lipid addition). Basal values were subtracted, and percentages were normalized to the maximum values obtained with 5 μM Iono. Data are presented as means ± SEMs (n=13 independent experiments for TRPC5-expressing cells, n=11

independent experiments for mock-transfected cells; n=11 independent experiments for TRPC6-expressing cells, n=8 independent experiments for mock-transfected cells. ~500—800 cells per group). **$p < 0.01$ and ***$p < 0.001$ (Mann-Whitney U test).

Fig. 5. Monitoring responses of photoreceptor cells stimulated with endocannabinoids and N-acyl glycine with GCaMP6f. (A, B) Representative GCaMP6f responses to 2-LG in control (*norpA*^{P24}) ommatidia (A) and in *norpA*^{P24};*trpl*^{302};*trp*^{343} ommatidia (B). The ommatidia were stimulated with 30 μM 2-LG, then with 5 μM ionomycin (Iono) to confirm GCaMP6f responsiveness in photoreceptor cells. The changes in fluorescence (gray scale levels 0—255) are shown in pseudo colors. The dotted lines in the images for basal conditions (before addition of 2-LG) outline individual rhabdomeres. 2-LG images were obtained at the 300 second time points in (C) and (D). Scale bars, 20 μm. **(C—F)** Traces showing representative $Ca^{2+}{}_i$ responses ($\Delta F/F_0$) in photoreceptor cells from control (*norpA*^{P24}) (C). *norpA*^{P24};*trpl*^{302};*trp*^{343} (D), *norpA*^{P24};+;*trp*^{343} (E) *norpA*^{P24};*trpl*^{302};+ (F) flies. The red and black bars indicate application of 30 μM 2-LG (60—300 seconds) and 5 μM ionomycin (after 300 seconds), respectively. **(G)** $\Delta F/F_0$ indicates the maximum $Ca^{2+}{}_i$ responses during the stimulation period (60—300 seconds) in (C) to (F) divided by basal fluorescence levels. **(H)** Quantification of area under curve during the stimulation period (60—300 seconds) in (C) to (F). Data are presented as means ± SEMs in G and H. n=9—11 independent experiments; 186—292 ommatidia per group. **$p < 0.01$. Kruskal-Wallis with Steel *post hoc* test. **(I)** Proportion of no or low responding photoreceptor

cells (max $\Delta F/F_0 \leq 0.2$) during the stimulation period in (C) to (F). Data are presented as means ± SEMs. n=9—11 independent experiments; 186—292 ommatidia per group. **p < 0.01, ***p < 0.001. One-way ANOVA with Tukey's *post hoc* analysis. **(J)** Traces showing representative $Ca^{2+}{}_i$ responses ($\Delta F/F_0$) in control (*norpA*^{P24}) photoreceptor cells in a bath containing 1.5 mM Ca^{2+} (blue in the bar near the top) or no Ca^{2+} (white in the bar near the top). The red and black bars indicate application of 30 μM 2-LG and 5 μM Iono, respectively. The dotted and solid orange lines indicate $\Delta F/F_0$ in a Ca^{2+}-containing bath in the absence (dotted) and presence (solid) of 2-LG. The dotted and solid green lines indicate $\Delta F/F_0$ in a bath without added Ca^{2+} in the absence (dotted) and presence (solid) of 2-LG. **(K)** Quantification of the maximum $Ca^{2+}{}_i$ responses to 30 μM 2-LG in the absence (-) or the presence (+) of 1.5 mM extracellular Ca^{2+}. $\Delta F/F_0$ in each Ca^{2+} condition was calculated using values in the periods indicated by green and orange dotted and solid lines in (J). Data are presented as means ± SEMs. n=8 independent experiments. Total: 211 ommatidia. ***p < 0.001. Paired Student's *t*-test. **(L)** Quantification of the maximum $Ca^{2+}{}_i$ responses to 30 μM 2-LG in the presence (+) or absence (-) of 10 μM ruthenium red (RuR). Maximum $Ca^{2+}{}_i$ responses in the presence of RuR (first 2 minutes) and after RuR washout (the following 3 minutes). Data are presented as means ± SEMs. n=9 independent experiments. Total: 238 ommatidia. ***p < 0.001. Paired Student's *t*-test. **(M, N)** Maximum $Ca^{2+}{}_i$ responses as measured by the GCaMP6f reporter of control (*norpA*^{P24}) and *norpA*^{P24};*trpl*^{302};*trp*^{343} photoreceptor cells to 100 μM LEA or 30 μM LinGly during the stimulation period (4 minutes). In the absence of the one outlier for LinGly, the significance is essentially unchanged (p=0.0097). Data

are presented as means ± SEMs. n=9—11 independent experiments. 175—325 ommatidia per group. **p < 0.01, ***p < 0.001. Unpaired Student's *t*-test for LEA and Mann-Whitney U test for LinGly.

Fig. 6 Monitoring GCaMP6f responses of photoreceptor cells stimulated with 2-LG and osmotic solutions. (A, B) Representative GCaMP6f responses to a hypotonic (~216 mOsm) solution in control (*norpA*^{P24}) ommatidia (A) and *norpA*^{P24};*trpl*^{302};*trp*^{343} ommatidia (B). **(C)** $\Delta F/F_0$ indicates the maximum $Ca^{2+}{}_i$ responses during the stimulation period (60—300 seconds) in (A) and (B) divided by basal fluorescence levels. Data are presented as means ± SEMs. control, n=11 independent experiments, 302 total ommatidia; *norpA*^{P24};*trpl*^{302};*trp*^{343}, n=9 independent experiments, 202 total ommatidia. *p < 0.05. Unpaired Student's *t*-test. **(D)** Representative GCaMP6f responses to 2-LG in control ommatidia (*norpA*^{P24}) followed by a combination of 2-LG and a hypotonic solution. The red and blue bars indicate application of 30 μM 2-LG (60—300 seconds) and the hypotonic solution (~216 mOsm) (after 180 seconds), respectively. **(E)** Quantification of the maximum $Ca^{2+}{}_i$ responses of control ommatidia (*norpA*^{P24}) to a hypotonic solution alone, 30 μM 2-LG alone, or a combination of a hypotonic solution and 2-LG. Data are presented as means ± SEMs. n=11—12 independent experiments. 274—358 ommatidia per group. *p < 0.05, ***p < 0.001. One-way ANOVA with Tukey's *post hoc* analysis. **(F)** Representative GCaMP6f responses to 2-LG followed by a combination of 2-LG and hypertonic solution in control (*norpA*^{P24})ommatidia. The red

and magenta bars indicate application of 30 μM 2-LG (60—300 seconds) and hypertonic solution (~416 mOsm; after 180 seconds), respectively.

Fig. 7 Endocannabinoid 2-LG activates TRP and TRPL in concert with mechanical stimulation. Shown is the phototransduction cascade. Light (thunderbolt) activates rhodopsin, which in turn leads to exchange of GTP for GDP and activation of $G\alpha_q$. $G\alpha_q$-GTP activates PLC (NORPA), catalyzing the hydrolysis of phosphatidylinositol (4,5)-bisphosphate (PIP_2), and production of diacylglycerol (DAG), inositol trisphosphate (IP_3) and a proton (H^+). DAG has a smaller head group than PIP_2, causing a conformational change in the membrane (membrane deformation), which is proposed to mechanically activate TRP and TRPL (*27*). Production of 2-linoleoyl glycerol (2-LG) from DAG is catalyzed by a DAG lipase (DAGL) encoded by *inaE* (*38*). We propose that TRP and TRPL are activated through dual mechanisms: by direct binding of 2-LG to the channels and by membrane deformation resulting from conversion of PIP_2 to DAG.

Figure 1

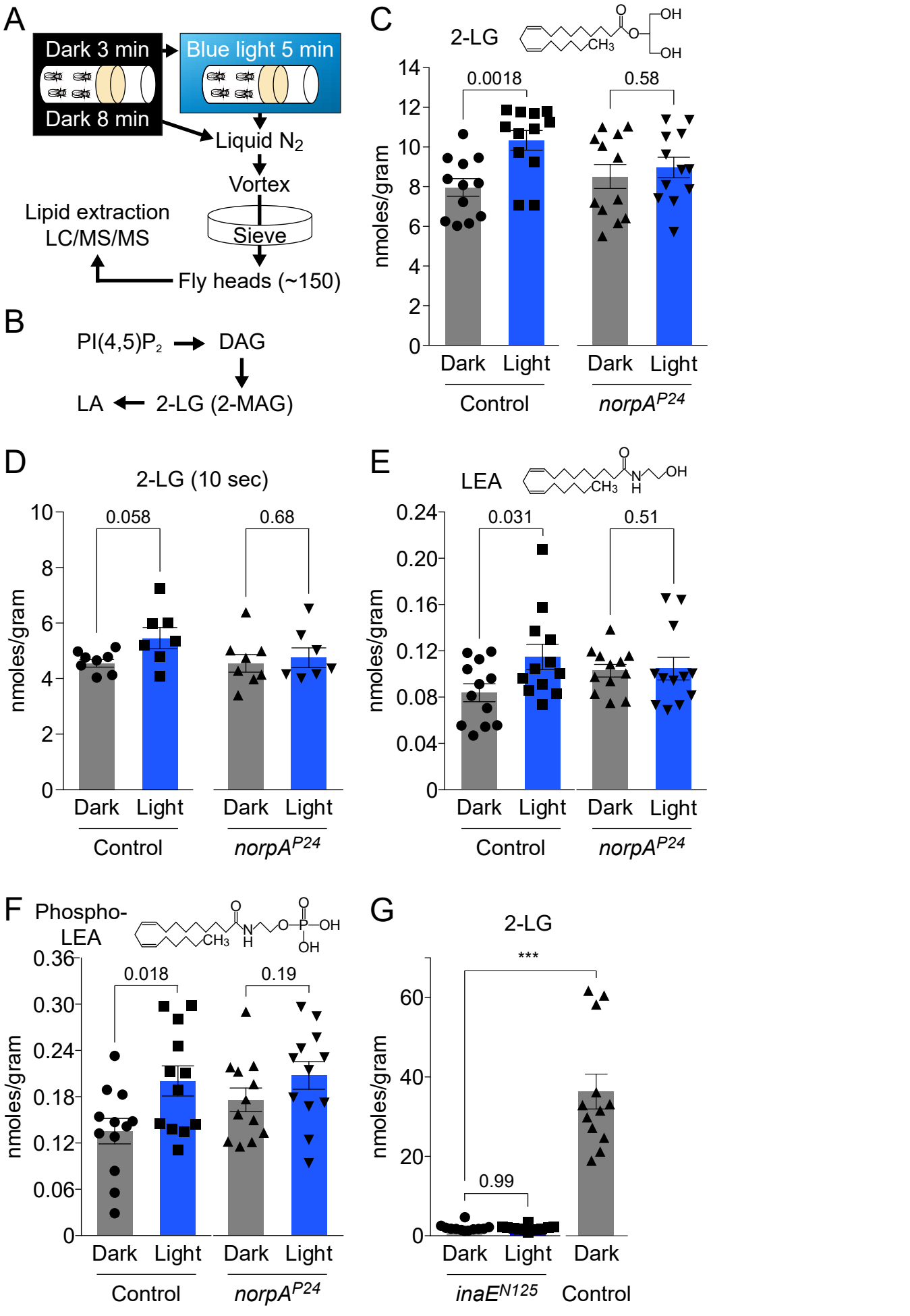
A
Dark 3 min
Dark 8 min
Blue light 5 min
Liquid N2
Vortex
Sieve
Lipid extraction
LC/MS/MS
Fly heads (~150)
B
PI(4,5)P2
DAG
LA
2-LG (2-MAG)
C
2-LG
0.0018
0.58
nmoles/gram
Dark
Light
Control
norpAP24
D
2-LG (10 sec)
0.058
0.68
E
LEA
0.031
0.51
F
Phospho-LEA
0.018
0.19
G
2-LG
***
0.99
inaEN125

Figure 2

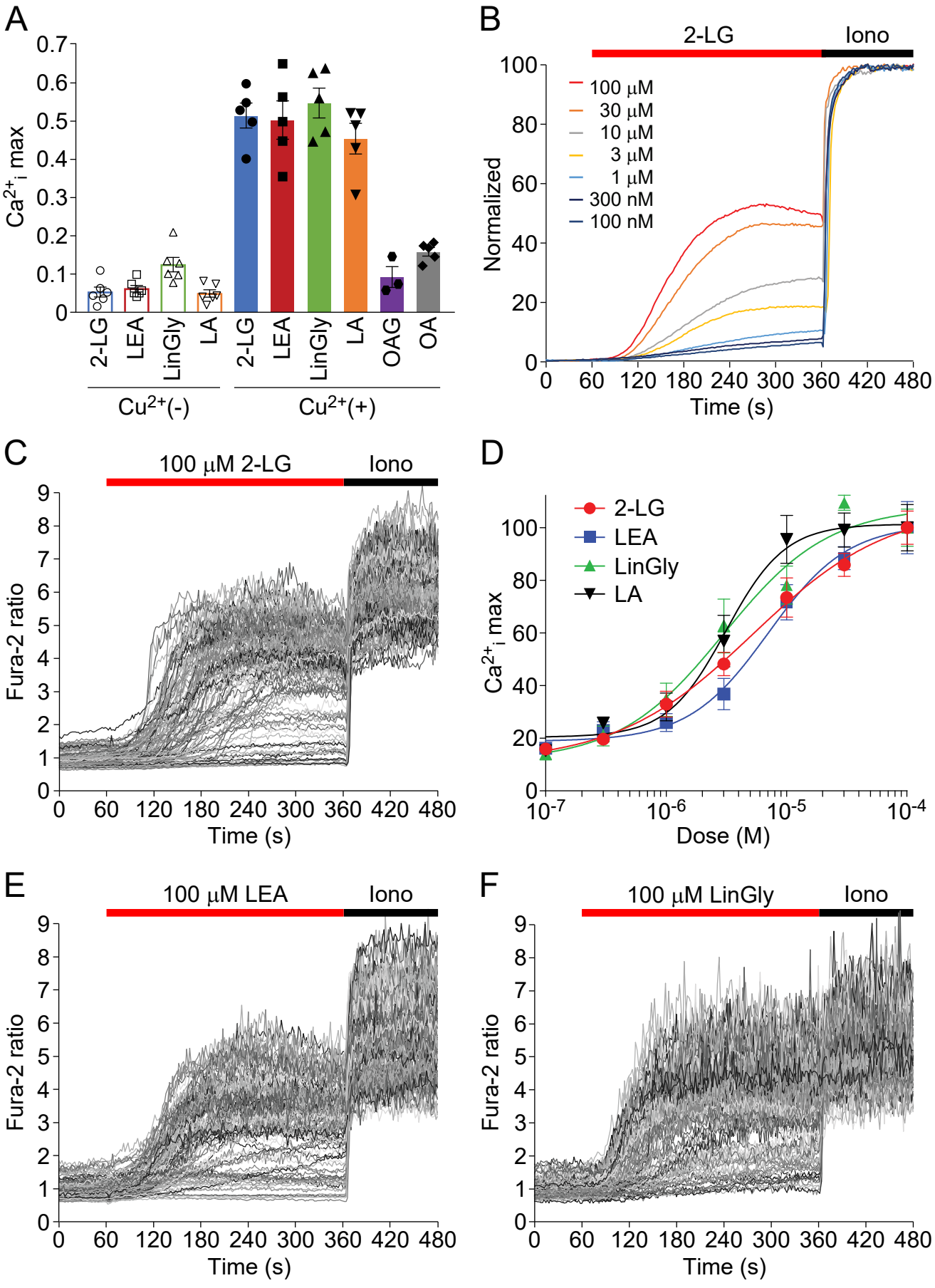
A
Ca^{2+}_i max
0.7
0.6
0.5
0.4
0.3
0.2
0.1
0
2-LG
LEA
LinGly
LA
2-LG
LEA
LinGly
LA
OAG
OA
Cu^{2+}(-)
Cu^{2+}(+)
B
2-LG
Iono
100 µM
30 µM
10 µM
3 µM
1 µM
300 nM
100 nM
Normalized
100
80
60
40
20
0
0 60 120 180 240 300 360 420 480
Time (s)
C
100 µM 2-LG
Iono
Fura-2 ratio
9
8
7
6
5
4
3
2
1
0
0 60 120 180 240 300 360 420 480
Time (s)
D
2-LG
LEA
LinGly
LA
Ca^{2+}_i max
100
80
60
40
20
0
10^{-7}
10^{-6}
10^{-5}
10^{-4}
Dose (M)
E
100 µM LEA
Iono
Fura-2 ratio
9
8
7
6
5
4
3
2
1
0
0 60 120 180 240 300 360 420 480
Time (s)
F
100 µM LinGly
Iono
Fura-2 ratio
9
8
7
6
5
4
3
2
1
0
0 60 120 180 240 300 360 420 480
Time (s)

Figure 3

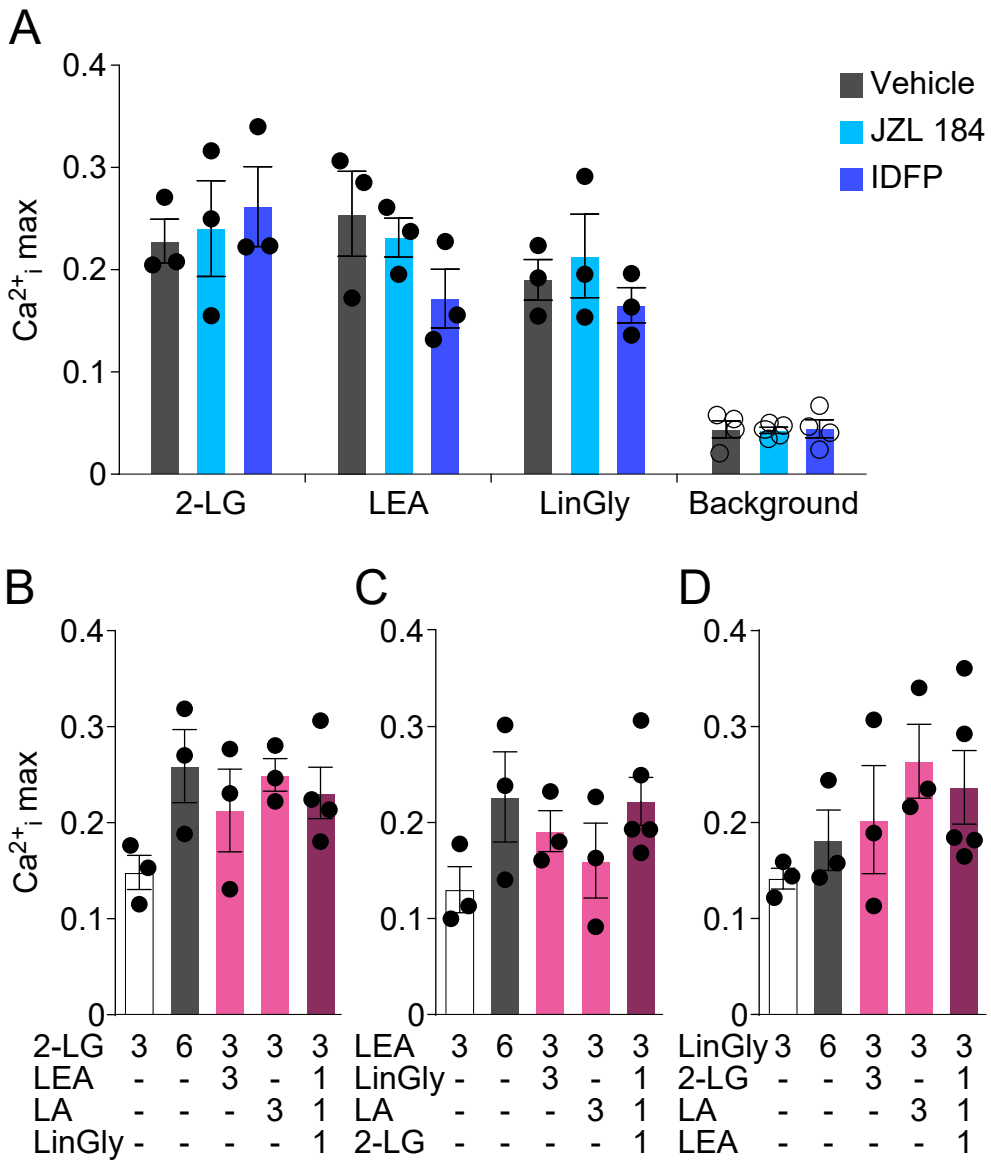
A
Vehicle
JZL 184
IDFP
Ca^{2+}_i max
0.4
0.3
0.2
0.1
0
2-LG
LEA
LinGly
Background
B
C
D
2-LG 3 6 3 3 3
LEA - - 3 - 1
LA - - - 3 1
LinGly - - - - 1
LEA 3 6 3 3 3
LinGly - - 3 - 1
LA - - - 3 1
2-LG - - - - 1
LinGly 3 6 3 3 3
2-LG - - 3 - 1
LA - - - 3 1
LEA - - - - 1

Figure 4

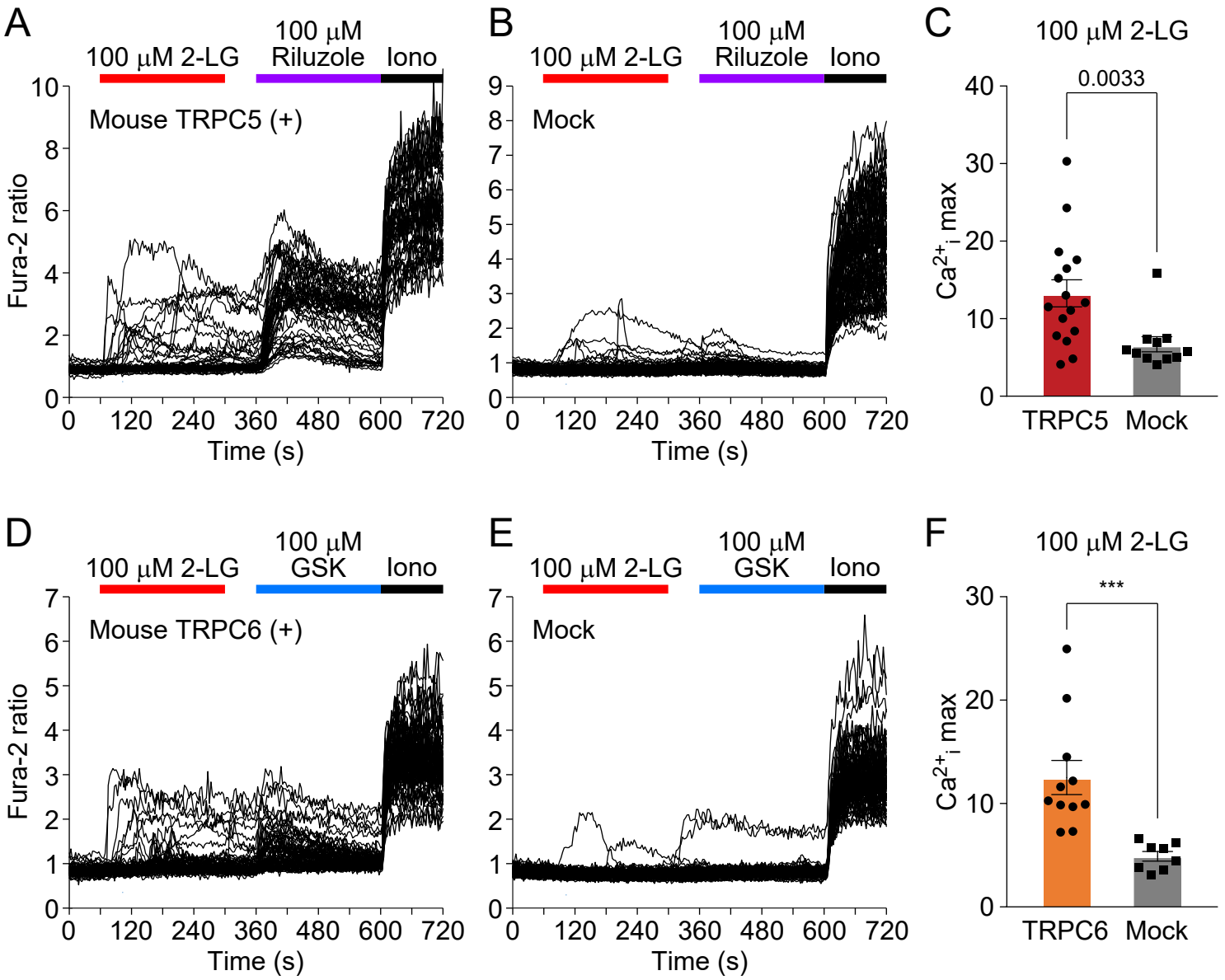
A
100 μM 2-LG
100 μM Riluzole
Iono
Mouse TRPC5 (+)
Fura-2 ratio
Time (s)
B
100 μM 2-LG
100 μM Riluzole
Iono
Mock
Time (s)
C
100 μM 2-LG
0.0033
Ca2+i max
TRPC5
Mock
D
100 μM 2-LG
100 μM GSK
Iono
Mouse TRPC6 (+)
Fura-2 ratio
Time (s)
E
100 μM 2-LG
100 μM GSK
Iono
Mock
Time (s)
F
100 μM 2-LG
***
Ca2+i max
TRPC6
Mock

Figure 5

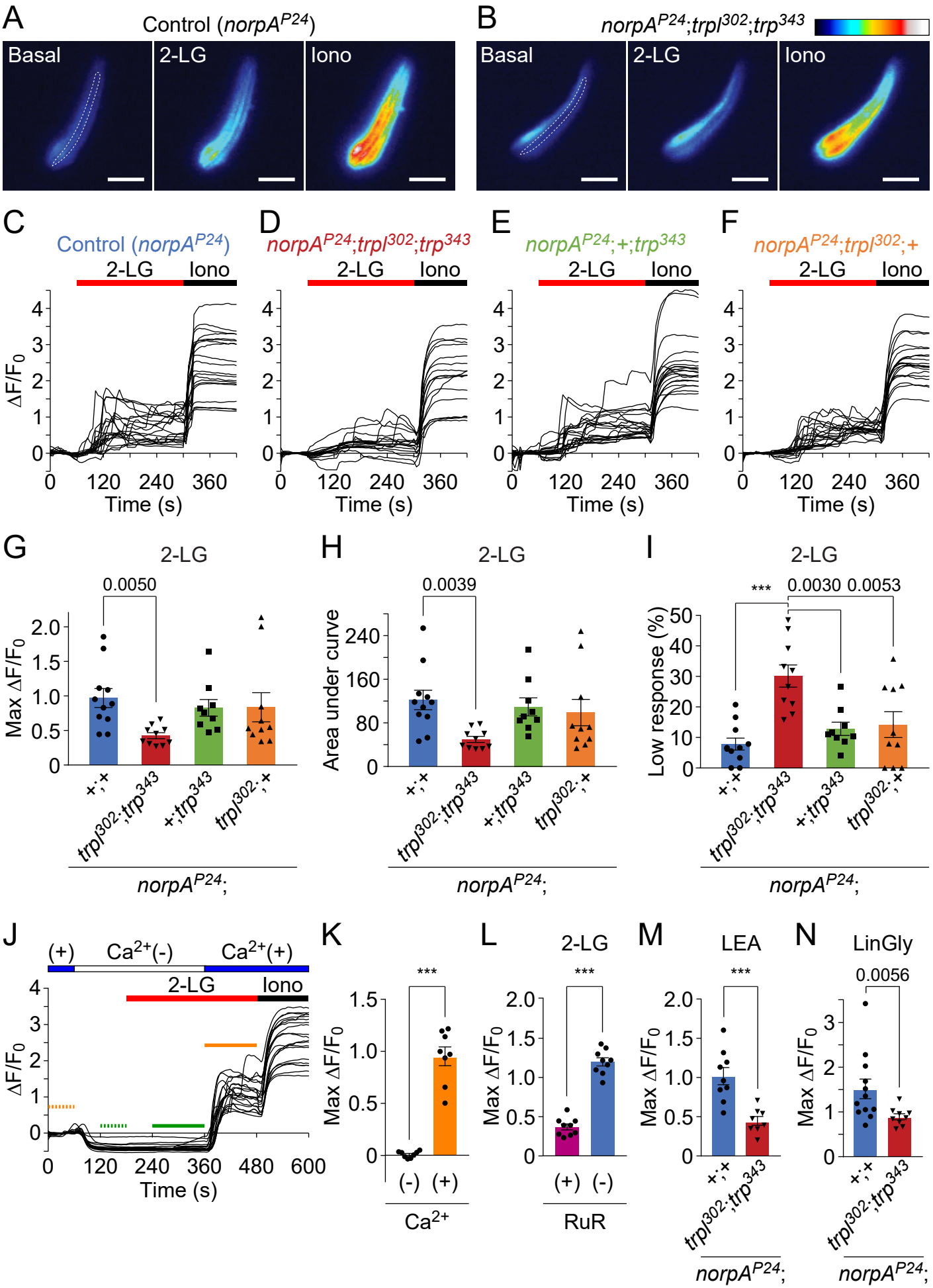
A
Control (norpA^P24)
Basal
2-LG
Iono
B
norpA^P24;trpl^302;trp^343
Basal
2-LG
Iono
C
Control (norpA^P24)
2-LG
Iono
ΔF/F0
Time (s)
D
norpA^P24;trpl^302;trp^343
2-LG
Iono
Time (s)
E
norpA^P24;+;trp^343
2-LG
Iono
Time (s)
F
norpA^P24;trpl^302;+
2-LG
Iono
Time (s)
G
2-LG
0.0050
Max ΔF/F0
+;+
trpl^302;trp^343
+;trp^343
trpl^302;+
norpA^P24;
H
2-LG
0.0039
Area under curve
+;+
trpl^302;trp^343
+;trp^343
trpl^302;+
norpA^P24;
I
2-LG
***
0.0030
0.0053
Low response (%)
+;+
trpl^302;trp^343
+;trp^343
trpl^302;+
norpA^P24;
J
(+)
Ca2+(-)
Ca2+(+)
2-LG
Iono
ΔF/F0
Time (s)
K
***
Max ΔF/F0
(-)
(+)
Ca2+
L
2-LG
***
Max ΔF/F0
(+)
(-)
RuR
M
LEA
***
Max ΔF/F0
+;+
trpl^302;trp^343
norpA^P24;
N
LinGly
0.0056
Max ΔF/F0
+;+
trpl^302;trp^343
norpA^P24;

Figure 6

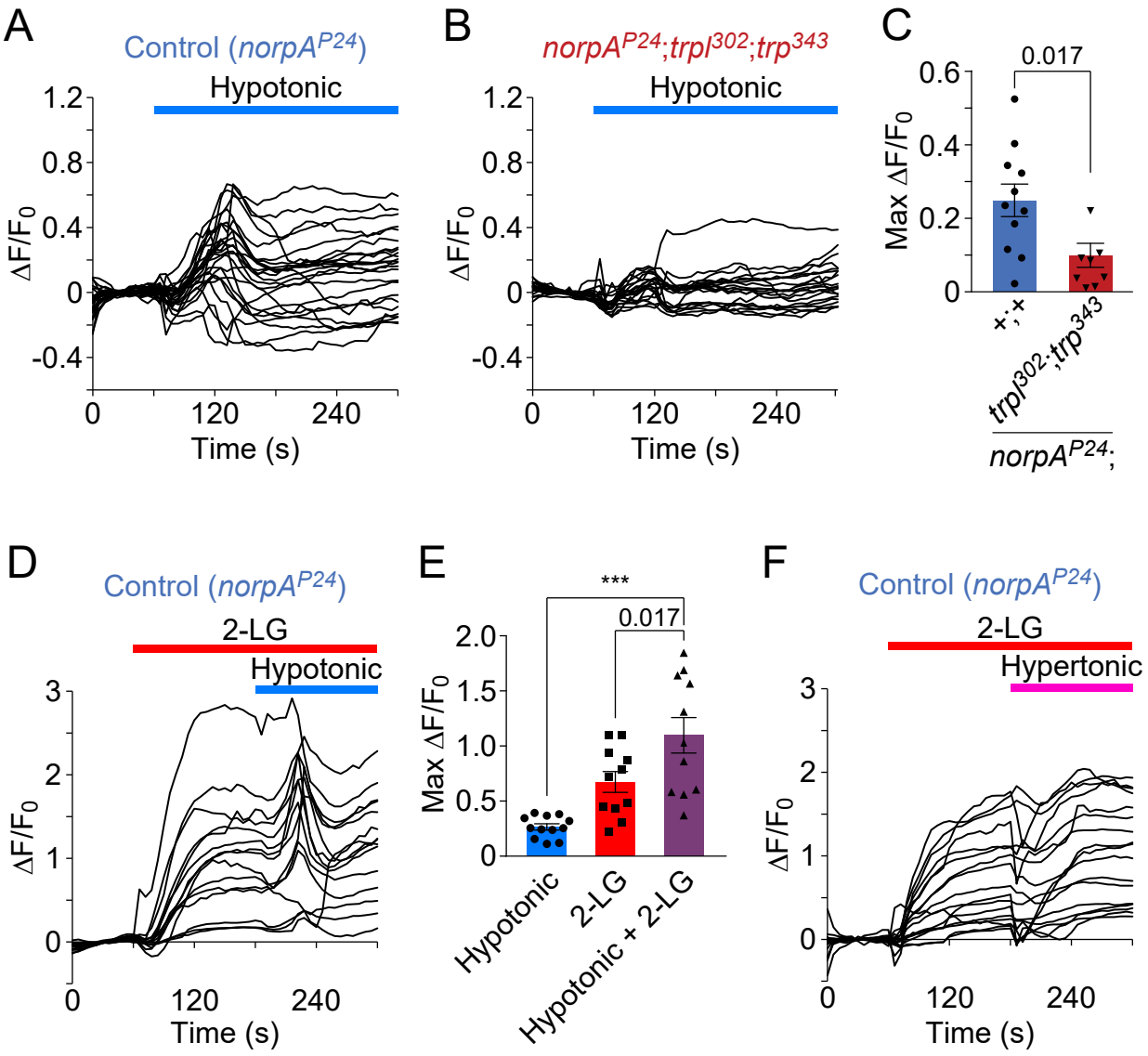
A
Control (norpA^P24)
Hypotonic
ΔF/F0
Time (s)
B
norpA^P24;trpl^302;trp^343
Hypotonic
ΔF/F0
Time (s)
C
0.017
Max ΔF/F0
+;+
trpl^302;trp^343
norpA^P24;
D
Control (norpA^P24)
2-LG
Hypotonic
ΔF/F0
Time (s)
E
***
0.017
Max ΔF/F0
Hypotonic
2-LG
Hypotonic + 2-LG
F
Control (norpA^P24)
2-LG
Hypertonic
ΔF/F0
Time (s)

Figure 7

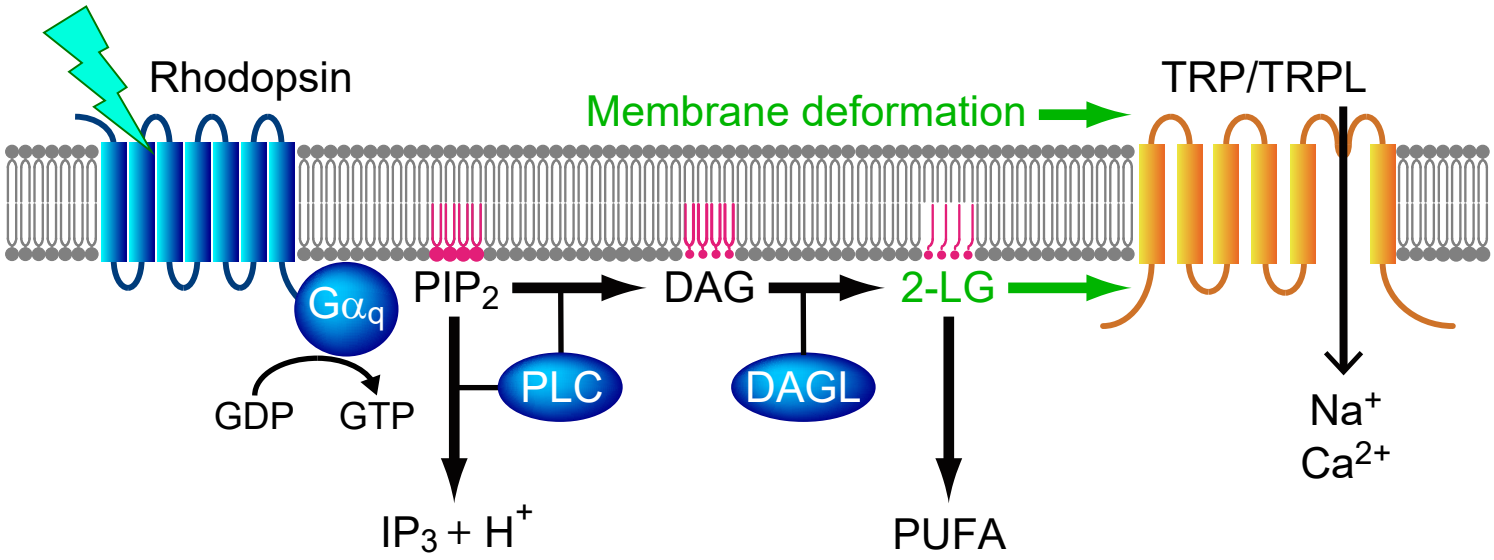
Rhodopsin
Membrane deformation
TRP/TRPL
Gαq
PIP2
DAG
2-LG
GDP
GTP
PLC
DAGL
Na+
Ca2+
IP3 + H+
PUFA

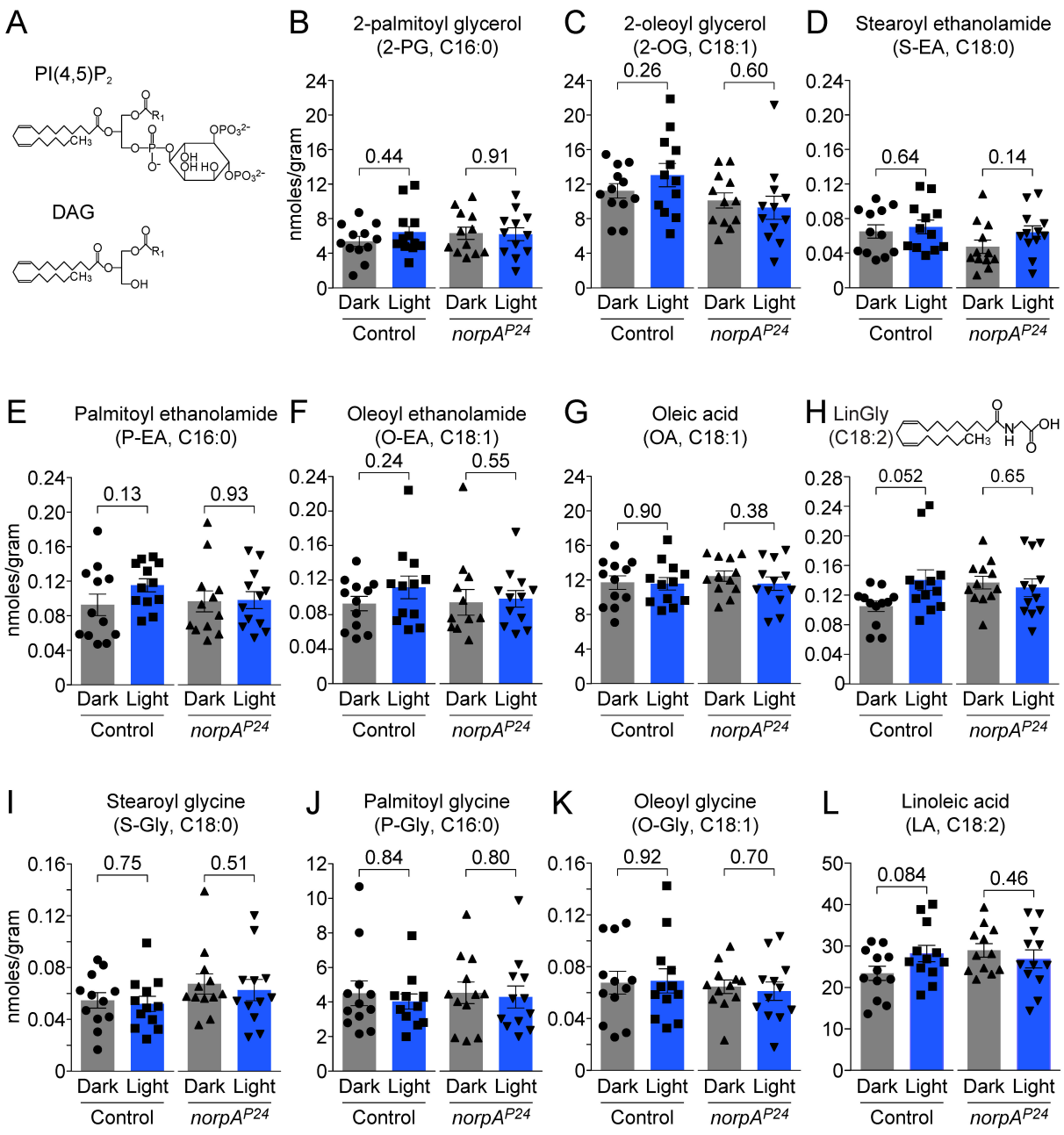

Fig. S1. Relative lipid levels in control (*w*^{1118}) and *norpA*^{P24} (in a *w*^{1118} background) heads from flies maintained in the dark and after light exposure. (**A**) The structures of phosphatidylinositol 4,5-bisphosphate [PI(4,5)P_2] and diacylglycerol (DAG are shown. (**B** to **L**) The amounts of the lipid metabolites 2-palmitoyl glycerol (2-PG) (B), 2-oleoyl glycerol (2-OG) (C), stearoyl ethanolamide (S-EA) (D), palmitoyl ethanolamide (P-EA) (E), oleoyl ethanolamide (O-EA) (F), oleic acid (OA) (G), linoleoyl glycine (LinGly) (H), stearoyl glycine (S-Gly) (I), palmitoyl glycine (P-Gly) (J), oleoyl glycine (O-Gly) (K), and linoleic acid (LA) (L) were measured (nmoles/gram) in the same set of samples used in Fig. 1. Data are presented as means

± SEMs. n=12 independent experiments; ~1,800 fly heads per group. Unpaired Student's *t*-tests or Mann-Whitney U test.

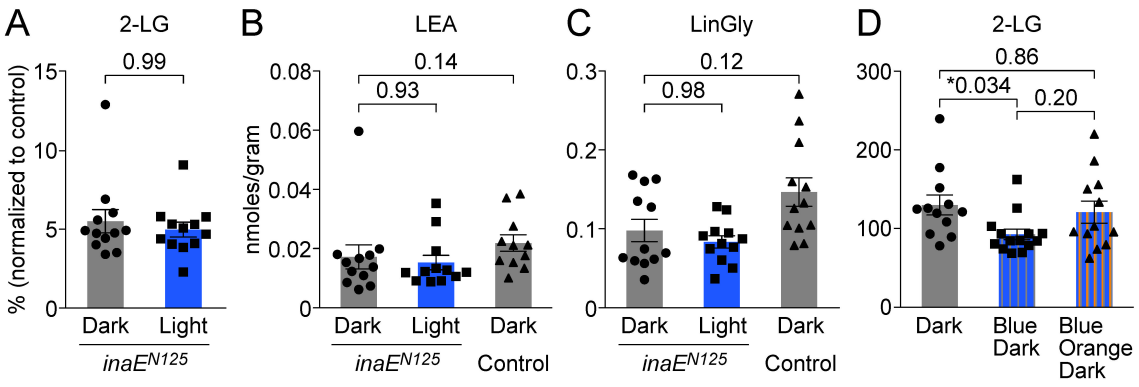

Fig. S2. Relative lipid levels in heads from *inaE*^{N125} and control (*w*^{1118}) flies maintained in the dark only or after light exposure.
(**A** to **C**) The amounts of the lipid metabolites 2-LG in *inaE*^{N125} flies normalized to that in the control in Fig. 1G (A), LEA in *inaE*^{N125} and control flies (B). and LinGly after 5-min blue light exposure in *inaE*^{N125} and control flies (C) were measured using the same set of samples used in Fig. 1G. The flies were either kept in the dark or exposed to blue light for 5 min. Data in (A) to (C) are presented as means ± SEMs. n=12 independent experiments; ~1,800 fly heads per group. Kruskal-Wallis test with a Steel *post hoc* test. **(D)** Concentrations (nmoles/gram) of 2-LG extracted from control heads that were maintained in the dark or exposed to 6 min of blue light then put in darkness, or exposed to 5 min of blue light, 1 min of orange light and then darkness. The difference in the concentration of 2-LG from Fig. 1C is due to modifications in the LC/MS/MS system. Data are presented as means ± SEMs. n=12—14 independent experiments; ~1,800—2,100 fly heads per group. Kruskal-Wallis test with a Steel-Dwass *post hoc* test.

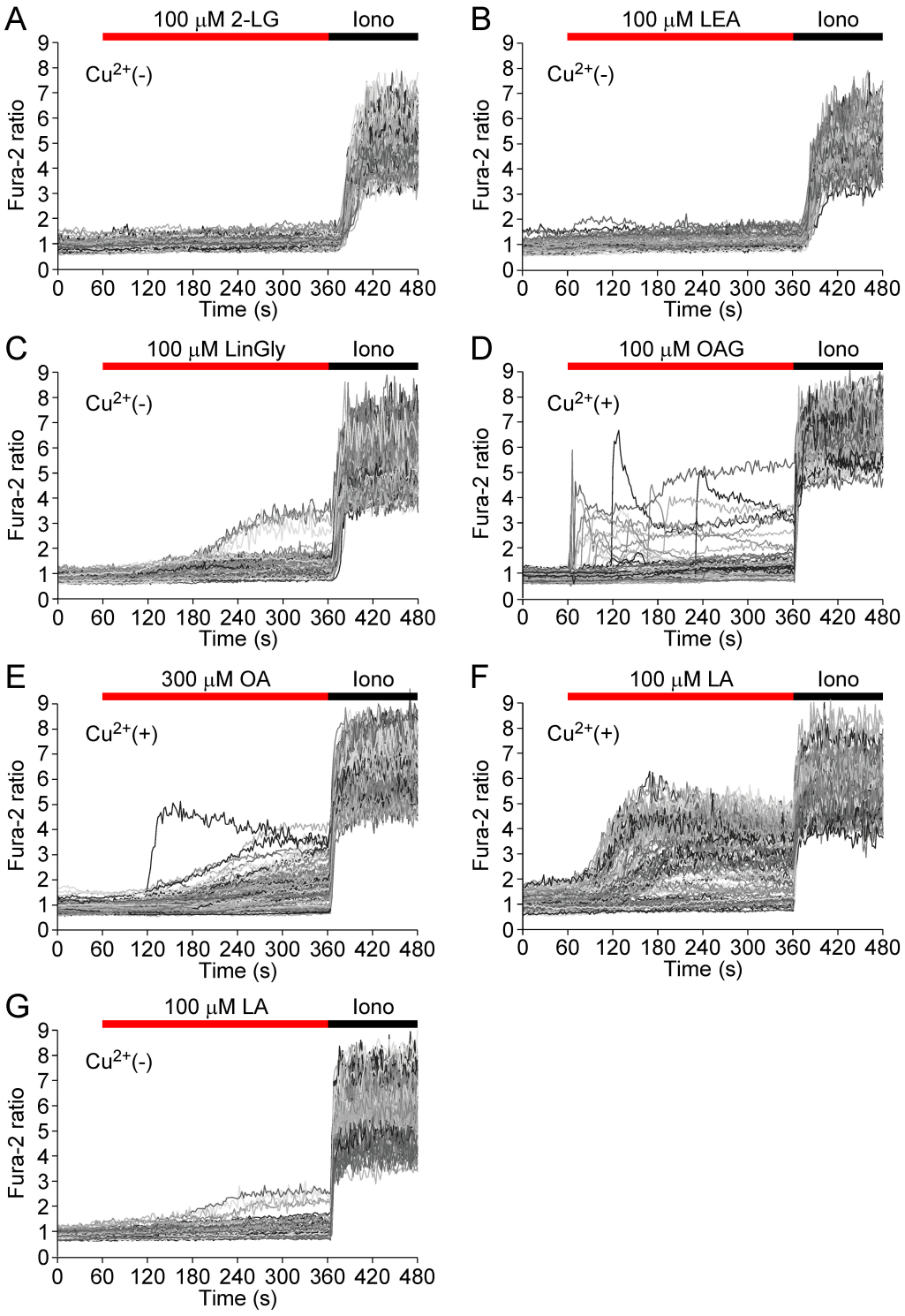

Fig. S3. Effects of linoleoyl-conjugates and linoleic acid on S2 cells.
(**A** to **G**) *trpl* was not induced [Cu^{2+} (-), (A—C and G)] or *trpl* was induced with Cu^{2+} (D—F) in S2 cells with $CuSO_4$-inducible expression of *trpl::GFP*. Cells were loaded with

Fura-2 AM and lipids (100 μM or 300 μM) were applied exogenously by perfusion. Ionomycin (Iono; 5 μM) was used to confirm cell viability. The red and black bars indicate the addition of the lipids or Iono, respectively. Representative Fura-2 responses in cells not expressing TRPL and treated with 2-LG (A), LEA (B), LinGly (C), or LA (G) and in TRPL-expressing cells and treated with OAG (D), OA (E), or LA (F) are shown. n=3—6 independent experiments; ~300—600 cells per group.

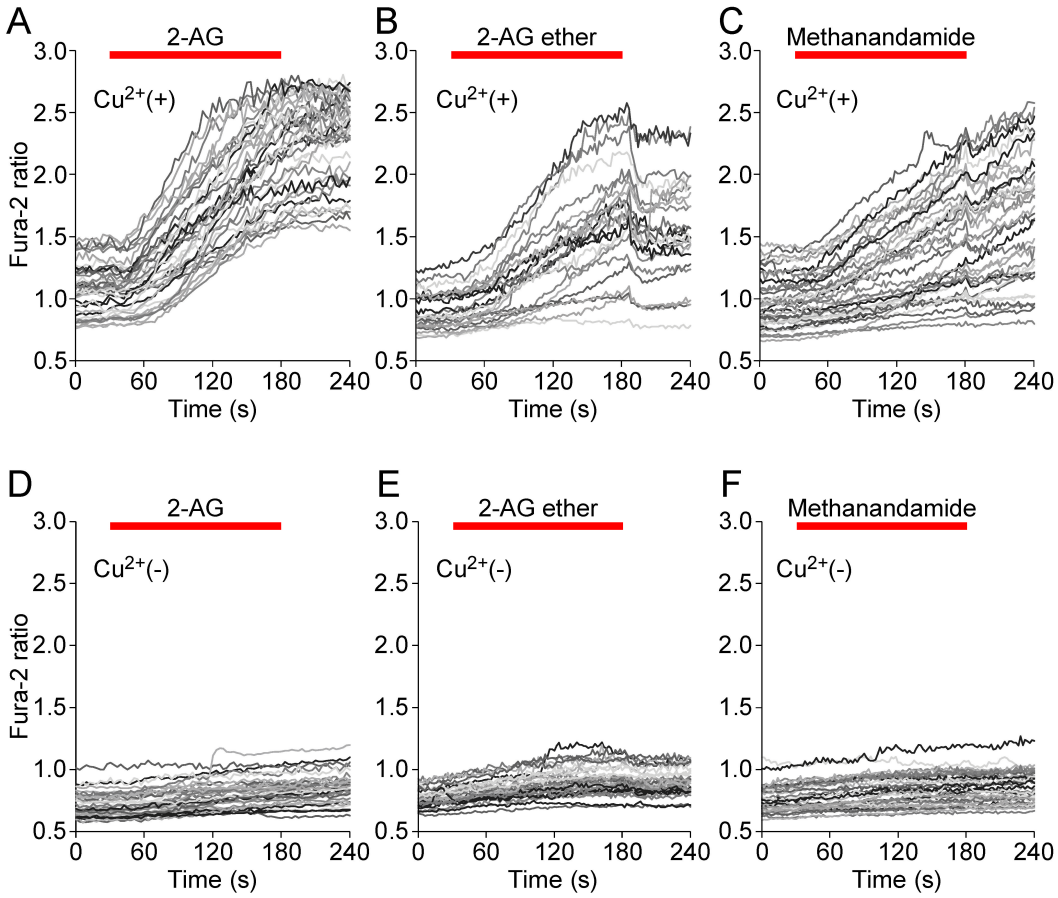

Fig. S4. Effects of endocannabinoid analogs on TRPL-expressing S2 cells. (**A** to **F**) *trpl* was induced with Cu^{2+} (A—C) or *trpl* was not induced [Cu^{2+} (-), (D—F)] in S2 cells with $CuSO_4$-inducible expression of *trpl::GFP*. The red bars indicate the addition of 100 μM of the indicated lipids by perfusion. Representative Fura-2 responses in TRPL-expressing cells and treated with 2-arachidonoyl glycerol (2-AG) (A), 2-AG ether (B), or methanandamide (C) and cells not expressing TRPL and treated with 2-AG (D), 2-AG ether (E), or methanandamide (F) are shown. n=3—4 independent experiments; ~120—300 cells per group).

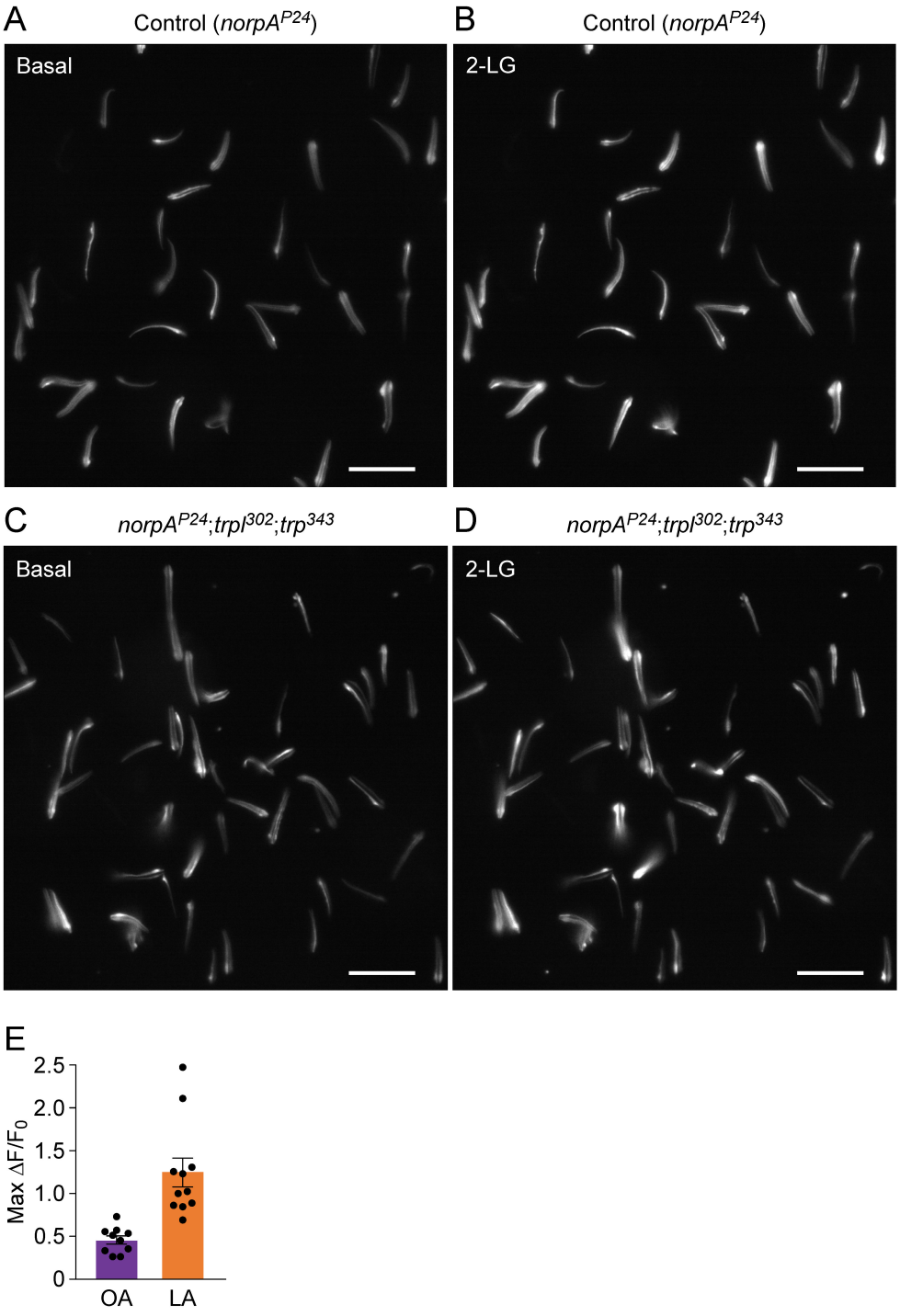

Fig. S5. GCaMP6f responses of photoreceptor cells in isolated ommatidia after addition of 2-linoleoyl glycerol (2-LG), oleic acid (OA) or linoleic acid (LA). Ommatidia were isolated from *ninaE>GCaMP6f* flies. Scale bars, 100 μm. **(A)** GCaMP6f fluorescence in control (*norpA*^{P24}) ommatidia before addition of 30 μM 2-LG. **(B)**

GCaMP6f fluorescence in control ommatidia ~240 seconds after addition of 30 μM 2-LG. **(C)** GCaMP6f fluorescence in *norpA*^{P24};*trpl*^{302};*trp*^{343} ommatidia before addition of 30 μM 2-LG. **(D)** GCaMP6f fluorescence in *norpA*^{P24};*trpl*^{302};*trp*^{343} ommatidia ~240 seconds after addition of 30 μM 2-LG. **(E)** Maximum $Ca^{2+}{}_i$ responses as indicated by the GCaMP6f reporter of control (*norpA*^{P24}) ommatidia to 30 μM OA and 30 μM LA during the stimulation period (4 minutes). Data are presented as means ± SEMs. n=10—11 independent experiments: 232 and 327 ommatidia per OA group and LA group, respectively.